This is the peer-reviewed version of the following article:
Physical Chemistry Chemical Physics **2018**, *20*, 307–316. DOI: 10.1039/C7CP07057H,
which has been published in final form at
http://pubs.rsc.org/en/content/articlelanding/2017/cp/c7cp07057h#!divAbstract.
Contents: main text + supplementary information.
This article may be used for non-commercial purposes only.

PCCP

ARTICLE

Fluorescence quenching of the N-methylquinolinium cation by pairs of water or alcohol molecules

Received 00th January 20xx,
Accepted 00th January 20xx

DOI: 10.1039/x0xx00000x

www.rsc.org/

Flor Rodríguez-Prieto,*[a,b] Carlos Costa Corbelle,[b] Berta Fernández,[b] Jorge A. Pedro,[a] M. Carmen Ríos Rodríguez*[a,b] and Manuel Mosquera*[a,b]

The singlet excited-state of the N-methylquinolinium cation (**MQ**$^+$) is a strong oxidant commonly used as photosensitizer, whose fluorescence is therefore quenched by electron donors. Interestingly, the fluorescence of **MQ**$^+$ is also quenched by hydroxy compounds such as water and alcohols, more difficult to oxidize. We investigated the quenching mechanism of **MQ**$^+$ fluorescence by small amounts of water and alcohols in acetonitrile solution. The fluorescence intensities and lifetimes exhibited a nonlinear dependence on quencher concentration. We found evidence that emissive exciplexes **MQ**$^+$*-ROH are formed between the excited quinolinium and the hydroxy compounds. An accurate quantitative description of the results was obtained with a model in which the exciplex reacts with a second molecule of the hydroxy compound, which quenches the fluorescence. The rate constant of this process increased as the quencher ionization energy decreased. We showed also that a low basicity of the hydroxy compound inhibits the quenching process. These results are consistent with the existence of a concerted photoinduced proton-coupled electron transfer (PCET) involving an intermediate complex of the excited quinolinium with a H-bonded molecular pair of the hydroxy compounds. In these pairs, a water or alcohol molecule is able to donate an electron to the photoexcited quinolinium cation and a proton to the second H-bonded hydroxy molecule, showing an enhanced reducing power in comparison with the isolated molecule. The structure of the intermediate complex was investigated by high-level quantum mechanical calculations. At high water concentrations in acetonitrile/water mixtures, the quenching process is slowed down, indicating that higher water aggregates are less effective for a PCET process. The results obtained may be relevant to the study of water oxidation and electron transfer in biological systems.

Introduction

N-methylquinolinium (Chart 1) belongs to the family of quinolinium cations, which upon photoexcitation behave as potent oxidants and are commonly used as photocatalysts.[1, 2] Due to their strong electron-acceptor character in the first-excited singlet state, the fluorescence of quinolinium compounds is quenched by electron transfer from a variety of electron donors, at diffusion-controlled rate in the most favourable cases.[3-8] This feature has been used for physiological anion-sensing applications and to build highly sensitive fluorescent sensors.[7-12] Surprisingly, fluorescence quenching by harder-to-oxidize species like methanol and ethanol was also observed.[13] Additionally, quenching by water was also proposed to explain the fluorescence enhancement observed upon addition of ClO_4^- and HSO_4^- to aqueous solutions of quinolinium cations, through the protective effect of adduct formation.[13] However, no conclusive explanation was found about the nature of the process by which water and alcohols quench the fluorescence of quinolinium compounds, as an electron transfer from these hard-to-oxidize species seems unlikely. With the aim to unravel the quenching mechanism, we studied the fluorescence quenching of **MQ**$^+$ by water and aliphatic alcohols in acetonitrile solution. We chose this solvent because it is polar enough to dissolve the quinolinium salt and has a high resistance to oxidation. We report here the finding that a pair of water or alcohol molecules quench the excited cation, whereas a single molecule is unable to do so. We propose that a proton-coupled electron transfer process enhances the electron donating capability of the hydroxy compounds and brings about an electron-transfer process that is impossible for a single water or aliphatic alcohol molecule.

Electron transfer is frequently made possible by the rate increase brought about by photoexcitation of the reactants, though coupling proton and electron transfer, or other

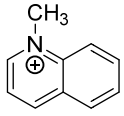

MQ$^+$

Chart 1 Molecular structure of N-methylquinolinium

[a]*Centro Singular de Investigación en Química Biolóxica e Materiais Moleculares (CIQUS), Universidade de Santiago de Compostela, E-15782 Santiago de Compostela, Spain*
E-mail: flor.rodriguez.prieto@usc.es, carmen.rios@usc.es, manuel.mosquera@usc.es
[b]*Departamento de Química Física, Facultade de Química, Universidade de Santiago de Compostela, E-15782 Santiago de Compostela, Spain*
† Electronic supplementary information (ESI) available: Kinetic model, supplementary experimental results and data analyses with supporting figures, and results of the ab initio calculations. See DOI: 10.1039/x0xx00000x

enhancement mechanisms.[14-18] Electronic excitation brings about a strong increase of molecular electron donor and acceptor abilities. Photoexcitation is therefore a method of choice to promote electron transfer processes, as it is also the coupling of electron and proton transfer, which catalyses redox processes by avoiding high-energy intermediates. PCET processes are at the heart of the most important chemical and biochemical energy conversion and storage processes, such as photosynthesis, respiration, and solar fuels.[16-23] The coordinated movement of electrons and protons is also implicated in other fundamental biological processes, like DNA mutation and repair, biological photoprotection mechanisms, and function of proteins.[15, 17, 21-25]

Photoinduced PCET processes combine the two above-mentioned enhancement mechanisms and lead therefore to large rate accelerations of electron transfer processes. This pattern is used by green plants in the photosynthetic process, and is also at the heart of many artificial photosynthesis schemes that pursue water splitting to form hydrogen and oxygen, or water reduction of CO_2 to carbon-based fuels.[16-23, 26, 27] Photoinduced PCET is therefore a cornerstone for the design of renewable energy-conversion systems, which, together with the need to understand the involvement of PCET in water and in biological systems, triggered an increasing interest in the study of its detailed mechanism from both the experimental and the theoretical points of view.[14-31]

In this paper, we report an in-depth quantitative investigation of the fluorescence quenching mechanism of the N-methylquinolinium cation by water and aliphatic alcohols in acetonitrile. The results provide evidence for a novel photoinduced PCET quenching mechanism, which involves an electron transfer from a pair of molecules of the hydroxy compounds to the photoexcited quinolinium. This knowledge will contribute to the understanding of biological processes and energy-converting systems where PCET involving hydroxy compounds plays a central role.

Experimental

Materials

N-Methylquinolinium iodide was prepared by the dropwise addition of a dilute solution of CH_3I in toluene over a solution of quinoline in toluene. After refluxing the mixture for 5 h, the solid obtained was filtered and washed with acetone. Solutions were made up in double-distilled water and in spectroscopy-grade solvents, and were not degassed. We employed N-methylquinolinium iodide solutions with concentrations of $\sim 10^{-4}$ mol dm^{-3} for absorption and fluorescence lifetimes measurements, and $\sim 10^{-5}$ mol dm^{-3} for steady-state fluorescence measurements. Chemicals were purchased from Sigma-Aldrich and used without further purification.

Absorption and fluorescence measurements

UV–vis absorption spectra were recorded in a Varian Cary 3E spectrophotometer. Fluorescence excitation and emission spectra were obtained in a Jobin-Yvon Spex Fluoromax-2 spectrofluorometer, with correction for instrumental factors by means of a reference photodiode and correction files supplied by the manufacturer. Fluorescence quantum yields were measured using quinine sulfate ($< 3 \times 10^{-5}$ mol dm^{-3}) in aqueous $HClO_4$ (1.0 mol dm^{-3}) as standard ($\Phi = 0.546$).[32, 33] To improve the accuracy of the quantum yields measurements, log-normal functions were fitted to the emission bands to evaluate the band areas.[34] All experiments were carried out at 20 ºC.

Fluorescence decays were measured by the time-correlated single-photon counting technique in an Edinburgh Instruments LifeSpec-ps time-resolved spectrometer equipped with a sub-nanosecond pulsed LED from PicoQuant as the excitation source (308 nm). The reconvolution analysis software supplied by the manufacturer was employed.

Data analyses and ab-initio calculations

Theoretical equations were fitted to the experimental data by means of a nonlinear weighted least-squares routine based on the Marquardt algorithm.[35] Principal-component global analyses were performed using a commercial software package (MATLAB for Windows, The MathWorks Inc., Natick, MA). The reported uncertainties correspond to the statistically estimated standard deviation of the measured quantities (type A standard uncertainty).[36] They are presented in parentheses after the estimated values of the measurands, referred to the corresponding last digits of the quoted results.[36]

MQ$^+$ has a iodide ion as counterion and this anion quenches its fluorescence at a diffusion-controlled rate.[4] The effect of the constant iodide concentration on **MQ$^+$** fluorescence is entirely negligible for the steady-state fluorescence measurements due to the low concentration used for these experiments ($\sim 10^{-5}$ mol dm^{-3}), but has a small effect that must be considered in the time-resolved experiments because of the 10-times higher concentration of the N-methylquinolinium iodide employed for these measurements. This small effect must be taken into account for the global analysis of steady-state and time-resolved measurements. For this reason, we have introduced in the analysis the linear dependence of the deactivation rate constant of excited **MQ$^+$** on iodide concentration in acetonitrile (quenching rate constant 5.22×10^{10} mol^{-1}dm^3 s^{-1}, measured for concentrations up to 2×10^{-4} mol dm^{-3}).

The ab-initio calculations were performed with the Gaussian 09 program package.[37]

Results and discussion

Kinetic analysis of the fluorescence quenching of MQ$^+$ by hydroxy compounds

The absorption spectra of **MQ$^+$** is almost identical in acetonitrile, water and the complete series of small aliphatic alcohols used in this work (see later). The fluorescence excitation spectra of **MQ$^+$** in acetonitrile, water, methanol, and ethanol were also almost identical, showed emission wavelength independence, and matched the first absorption

band (Fig. 1 and Fig. 1S–3S in the ESI†). The fluorescence emission spectra in the same solvents were independent of the excitation wavelength and very similar in aqueous solution and in acetonitrile, but exhibited a small red shift in methanol and ethanol (Fig. 1 and Fig. 4S, ESI†). The intensity, nevertheless, considerably declined in the series. The fluorescence quantum yield of **MQ**$^+$ decreased 2 times on going from acetonitrile to aqueous solution, and further diminished by a factor of 100 on going to methanol or ethanol solutions (Table 1). To get information on the fluorescence quenching mechanism, we studied the effect of small amounts of water and alcohols on the fluorescence of **MQ**$^+$ in acetonitrile solutions.

We investigated the decrease of the fluorescence intensity of **MQ**$^+$ in acetonitrile upon addition of water, methanol, ethanol, 1-propanol, 1,2-ethanediol, and 1,3-propanediol. Plots of the fluorescence intensity ratio in the absence and presence of quencher (F^0/F) versus quencher concentration showed nonlinear Stern–Volmer relationships with upward curvature in all cases (Fig. 2 and Fig. 5S–9S, ESI†). As can be seen from these plots, F^0/F gradually changed with the emission wavenumber, which revealed that the shape of the emission spectra changed with the addition of quenchers. These results suggest that a second fluorescent species is formed. This species must exist only in the excited state, as the excitation spectra remained unchanged in all cases upon addition of quenchers (cf. Fig. 2 and Fig. 5S–9S, ESI†).

To examine the possible effect of hydrogen bonding on the quenching process, we studied the influence of 2,2,2-trifluoroethanol on the fluorescence of **MQ**$^+$ solutions in acetonitrile. We chose this alcohol due to its extremely low hydrogen-bond basicity, originated by the strong electron-withdrawing effect of the fluorine atoms.[38, 39] We found that no fluorescence quenching at all was observed in the alcohol concentration range 0 to 0.39 mol dm^{-3} (Fig. 10S, ESI†).

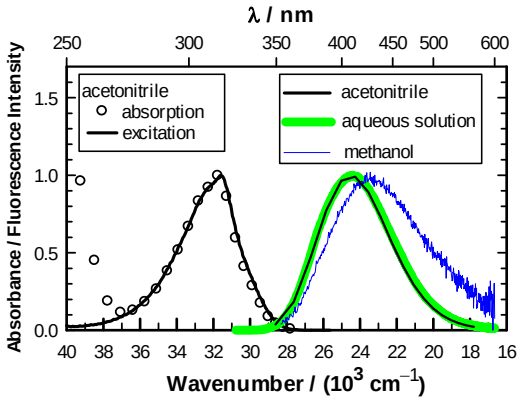

Fig. 1 Normalized absorption and fluorescence excitation spectra of **MQ**$^+$ in acetonitrile (left, $\tilde{\nu}_{em}$= 24630 cm^{-1}), together with the fluorescence emission spectra in aqueous solution, acetonitrile, and methanol (right, $\tilde{\nu}_{exc}$ = 31950 cm^{-1}).

Table 1 Fluorescence Quantum Yields Φ of **MQ**$^+$ in various solvents

Solvent	Φ
Acetonitrile	0.422
Water	0.232
Methanol	0.00398
Ethanol	0.00221

The fluorescence decay of **MQ**$^+$***** in acetonitrile in the absence of quenchers was monoexponential, with a lifetime of τ^0 = 23.37(4) ns. It remained monoexponential upon addition of hydroxy compounds (some examples are shown in Fig. 11S, ESI†), but the lifetime τ decreased as their concentration increased. Nonlinear Stern–Volmer plots of τ^0/τ versus quencher concentration were obtained in all cases, but their curvatures were significantly different from those obtained for the intensity ratio F^0/F (cf. Fig. 2 and Fig. 5S–9S, ESI†). This behaviour, together with the change of the spectral shape observed upon addition of hydroxy compounds, revealed that a quenching mechanism more complex than static and/or dynamic quenching must be operating.

Principal-component analysis applied to the series of fluorescence emission spectra of **MQ**$^+$ at different quencher concentrations showed that two independent spectral components are needed to reproduce the spectral series.[40, 41] This indicates that a new emissive species appears upon addition of quenchers, which we identify with an exciplex **E*** formed by the excited quinolinium cation and the quencher (see Scheme 1).

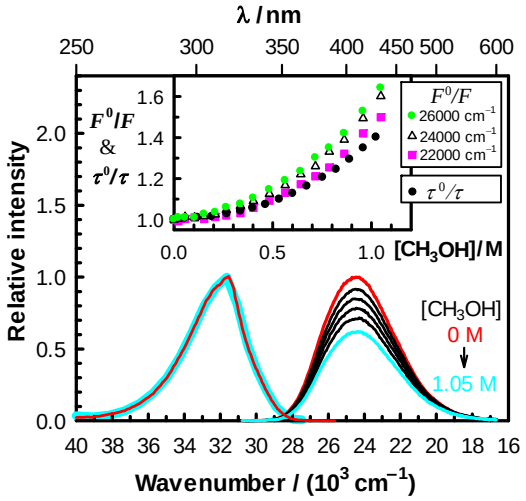

Fig. 2 Influence of methanol on the fluorescence spectrum of **MQ**$^+$ in acetonitrile. Left: Normalized fluorescence excitation spectra in neat acetonitrile (red thin line) and with addition of 1.05 mol dm^{-3} of methanol (cyan thick line), $\tilde{\nu}_{em}$ = 24630 cm^{-1}; Right: Fluorescence emission spectra with increasing concentration of methanol in the range 0 to 1.05 mol dm^{-3}, $\tilde{\nu}_{exc}$ = 31950 cm^{-1}. The inset shows the influence of methanol concentration on the fluorescence intensity ratio F^0/F at three emission wavenumbers, with $\tilde{\nu}_{exc}$ = 31950 cm^{-1}, and on the fluorescence lifetime ratio τ^0/τ, measured at $\tilde{\nu}_{exc}$ = 32540 cm^{-1} and $\tilde{\nu}_{em}$ = 24400 cm^{-1}.

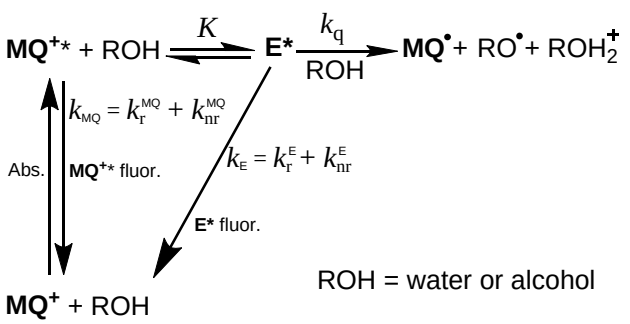

Scheme 1 Excitation and deactivation pattern proposed for **MQ**$^+$ in acetonitrile in the presence of water or alcohols

To explain the complex fluorescence intensity and lifetime dependence on quencher concentration (Fig. 2 and Fig. 5S–9S, ESI†), we propose that after excitation of **MQ**$^+$ and formation of the exciplex **E***, a second molecule of the hydroxy compound approaching **E*** induces its nonradiative deactivation. Furthermore, as the fluorescence decay of **MQ**$^+$* was monoexponential, we assume that a fast equilibrium is established between **MQ**$^+$* and **E***. To test the proposed mechanism, a thorough data analysis was carried out, as explained below.

Any emission spectrum $\boldsymbol{F}$ of the series must be a linear combination of the spectra of the emissive species **MQ**$^+$* and **E***. In eq 1, $\boldsymbol{F}^{\mathbf{0}}_{\mathrm{MQ}}$ and $\boldsymbol{F}^{\mathbf{0}}_{\mathrm{E}}$ represent the fluorescence spectra that would be obtained for **MQ**$^+$* and **E*** if each absorbed photon formed an excited molecule of the respective species, and only the unimolecular deactivation of these excited species would be operative (see the kinetic model, ESI†). The coefficients C_{MQ} and C_{E} are the contributions of **MQ**$^+$* and **E*** spectra to the experimental spectrum, and their values depend on the quencher concentration.

$$\boldsymbol{F} = C_{\mathrm{MQ}}\,\boldsymbol{F}^{\mathbf{0}}_{\mathrm{MQ}} + C_{\mathrm{E}}\,\boldsymbol{F}^{\mathbf{0}}_{\mathrm{E}} \qquad (1)$$

From the mechanism in Scheme 1, one can easily derive eqs 2 to 4, which show the predicted dependence on quencher concentration of the emission coefficients C_{MQ} and C_{E}, and of the lifetime ratio τ^0/τ (see the kinetic model in the ESI†).

$$C_{\mathrm{MQ}} = \frac{1}{1 + \frac{K\,k_{\mathrm{E}}}{k_{\mathrm{MQ}}}[\mathrm{ROH}] + \frac{K\,k_{\mathrm{q}}}{k_{\mathrm{MQ}}}[\mathrm{ROH}]^2} \qquad (2)$$

$$C_{\mathrm{E}} = \frac{\frac{K\,k_{\mathrm{E}}}{k_{\mathrm{MQ}}}[\mathrm{ROH}]}{1 + \frac{K\,k_{\mathrm{E}}}{k_{\mathrm{MQ}}}[\mathrm{ROH}] + \frac{K\,k_{\mathrm{q}}}{k_{\mathrm{MQ}}}[\mathrm{ROH}]^2} \qquad (3)$$

$$\frac{\tau^0}{\tau} = \frac{1 + \frac{K\,k_{\mathrm{E}}}{k_{\mathrm{MQ}}}[\mathrm{ROH}] + \frac{K\,k_{\mathrm{q}}}{k_{\mathrm{MQ}}}[\mathrm{ROH}]^2}{1 + K\,[\mathrm{ROH}]} \qquad (4)$$

In these equations (see Scheme 1), k_{MQ} and k_{E} are the unimolecular deactivation rate constants of the excited quinolinium cation and the exciplex, respectively. They correspond to the sum of the radiative k_{r} and the nonradiative k_{nr} deactivation constants of the respective species. k_{q} represents the quenching rate constant of the exciplex by ROH, K is the exciplex formation equilibrium constant, and τ^0 is the lifetime of **MQ**$^+$* in the absence of quenchers.

For each quencher, we analysed by Principal-Component Global Analysis (PCGA),[40, 41] with the set of eqs 1 to 4, the series of fluorescence spectra and lifetimes of **MQ**$^+$ obtained at different quencher concentrations. From these analyses, we obtained the fluorescence spectra $\boldsymbol{F}^{\mathbf{0}}_{\mathrm{MQ}}$ and $\boldsymbol{F}^{\mathbf{0}}_{\mathrm{E}}$, together with the optimized values of K, k_{MQ}, k_{E}, and k_{q}, collected in Table 2. Fig. 3 shows graphically the fit results obtained for methanol: part (A) displays the optimized spectra $\boldsymbol{F}^{\mathbf{0}}_{\mathrm{MQ}}$ and $\boldsymbol{F}^{\mathbf{0}}_{\mathrm{E}}$, and parts (B), (C) and (D) show the experimental fluorescence lifetimes τ and the coefficients C_{MQ} and C_{E} as a function of quencher concentration, together with plots of the fitted curves calculated with the single set of parameters shown in Table 2. It is seen that the model quantitatively reproduces the fluorescence intensity and lifetime data. The same goodness of

Table 2 Fluorescence quenching parameters[a] obtained by PCGA for **MQ**$^+$ in acetonitrile in the presence of quenchers of different ionization energy (E_{i}): ratio of **MQ**$^+$ fluorescence quantum yield Φ^0_{MQ} and exciplex fluorescence efficiency η^0_{E}, and equilibrium and rate constants defined in Scheme 1.

Quencher	E_{i}/eV	$\frac{\Phi^0_{\mathrm{MQ}}}{\eta^0_{\mathrm{E}}}$	η^0_{E}	$\frac{K}{\mathrm{mol^{-1}dm^3}}$	$\frac{k_{\mathrm{MQ}}}{10^7\mathrm{s^{-1}}}$	$\frac{k_{\mathrm{E}}}{10^7\mathrm{s^{-1}}}$	$\frac{k_{\mathrm{q}}}{10^8\mathrm{mol^{-1}dm^3s^{-1}}}$	$\frac{k_{\mathrm{r}}^{\mathrm{E}}}{10^7\mathrm{s^{-1}}}$	$\frac{k_{\mathrm{nr}}^{\mathrm{E}}}{10^7\mathrm{s^{-1}}}$
water	12.62[b]	0.83	0.51	0.217(5)	4.41(3)	2.81(5)	0.250(3)	1.4	1.4
2,2,2-trifluoroethanol	11.49[b]	–	–	–	–	–	–	–	–
methanol	10.84[b]	0.56	0.75	0.112(3)	4.35(1)	2.6(1)	1.90(4)	2.0	0.6
ethanol	10.48[b]	1.9	0.22	0.123(5)	4.33(2)	8.1(3)	6.5(2)	1.8	6.3
1-propanol	10.22[b]	2.4	0.18	0.115(6)	4.35(1)	10.4(6)	9.0(4)	1.8	8.6
1,2-ethanediol	10.16[b]	5.8	0.073	0.28(2)	4.34(1)	24(1)	6.2(3)	1.7	22
1,3-propanediol	9.7[c]	3.2	0.13	0.169(5)	4.34(1)	16.9(7)	12.1(5)	2.2	14.7

[a] T = 293 K. [b] From ref.[42] [c] From ref.[43]

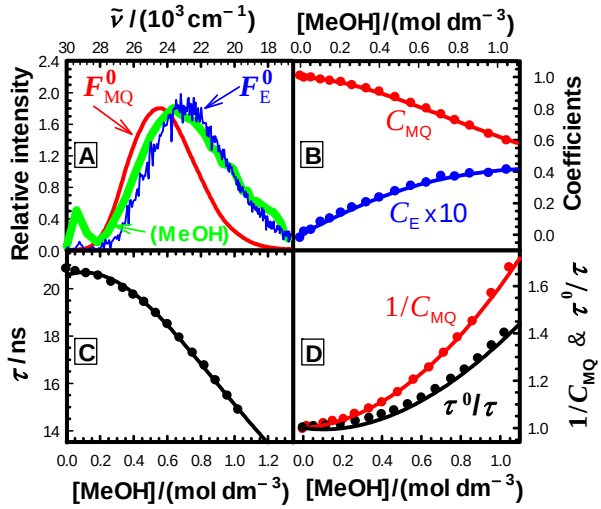

Fig. 3 Results of the principal-component global analysis of the fluorescence spectra and lifetimes of **MQ**$^+$ in acetonitrile in the presence of methanol: (A) Normalized component spectra obtained, associated to **MQ**$^+$***** ($\boldsymbol{F}^0_{MQ}$, red line) and the exciplex ($\boldsymbol{F}^0_E$, blue line), together with the fluorescence spectrum of **MQ**$^+$ in neat methanol ($\tilde{\nu}_{exc}$ = 31950 cm^{-1}, green line, with solvent Raman band); (B) the coefficients C_{MQ} and C_E representing the contributions of the **MQ**$^+$***** and **E*** spectra to the experimental spectrum, and the fit lines; (C) the experimental fluorescence lifetimes and the fit line; (D) the experimental values of $1/C_{MQ}$ and τ^0/τ, and the calculated fits.

fit was obtained for water and the rest of the alcohols investigated (Fig. 12S–16S, ESI†), which reflects the model consistency.

We show in Fig. 3(A) that the fluorescence spectrum recorded for **MQ**$^+$ in neat methanol almost completely overlaps with the spectrum $\boldsymbol{F}^0_E$ obtained by PCGA for the exciplex **MQ**$^+$*****–methanol in acetonitrile (the same is also true for ethanol, see Fig. 13S, ESI†). We interpret this fact as an indication that the exciplex is the main emissive species in pure methanol, favoured by the high concentration of the solvent.

The integrated areas of the fluorescence spectra $\boldsymbol{F}^0_{MQ}$ and $\boldsymbol{F}^0_E$ obtained from PCGA contain information on the quantum yields of these species in the solvent used, acetonitrile. The ratio of the areas equals the quotient Φ^0_{MQ}/η^0_E, where Φ^0_{MQ} denotes the fluorescence quantum yield of **MQ**$^+$ in acetonitrile in the absence of quencher, and η^0_E represents the fluorescence quantum efficiency of **E*** if only the unimolecular photophysical deactivation of this excited species would be operative ($\eta^0_E = k^E_r/k_E$, see details in the Supporting Information). The values of Φ^0_{MQ}/η^0_E for various quenchers are collected in Table 2. As Φ^0_{MQ} is the fluorescence quantum yield of **MQ**$^+$ in neat acetonitrile (0.422), the values of η^0_E for the different exciplexes in this solvent can be calculated, together with their radiative and nonradiative deactivation constants (Table 2). For water and methanol, the η^0_E value is slightly greater than Φ^0_{MQ}, which means that for these species, the fluorescence quenching is entirely due to the bimolecular reaction process with a second molecule of the hydroxy compound. For the rest of the alcohols, η^0_E is somewhat lower than Φ^0_{MQ}, but the main quenching comes also from the bimolecular deactivation process with rate constant k_q (compare for example the results obtained on going from water to 1,3-propanediol: a 4-fold decrease of η^0_E but almost a 50-fold increase in the bimolecular quenching rate constant k_q). Therefore, we conclude that the main process responsible for the strong fluorescence quenching observed is not the formation of the exciplex, but its bimolecular quenching by a second molecule of the hydroxy compound. In the following, we discuss the nature of this quenching process.

Involvement of an electron transfer process in the quenching mechanism

Quinolinium cations are strong electron-acceptor photosensitizers, whose fluorescence has been shown to be quenched by low concentrations of anions through a dynamic electron-transfer mechanism.[4, 8] In this work, we show that water and aliphatic alcohols exhibit a much lower quenching efficiency of **MQ**$^+$ fluorescence and a more complex mechanism compared to the anions. If an electron transfer is involved in this quenching process, its efficiency must increase with the ease of oxidation of the quencher. As the standard electrode potentials E^0 are not known for all quenchers, we used the gas-phase ionization energies (E_i), linearly correlated with E^0,[44] as a measure of their ability to donate an electron. The data presented in Table 2 suggest that an electron transfer may be involved in the quenching process, as a trend of increasing the quenching rate constant with decreasing ionization energy of the quencher is observed, and a linear correlation exists between log k_q and E_i (Fig. 4). Nevertheless, the process is not a simple dynamic quenching as for the anions,[4, 8] as could be anticipated by the more difficult alcohol and water oxidation. Even for stronger oxidants like photoexcited methyl viologen (MV^{2+}*****), an endergonic process was predicted for electron transfer from water[45] (reduction potentials $E^0(MV^{2+}*/MV^{\bullet+})$ = 3.65 V vs NHE,[45] much higher than E^0(**MQ**$^+$***/MQ**$^\bullet$) = 2.9 V vs NHE).[3] This is corroborated by our results, as the reaction of **MQ**$^+$***** with water to form the exciplex does not quench the fluorescence of **MQ**$^+$***** (η^0_E = 0.51, slightly greater than Φ^0_{MQ} = 0.422), as expected for a very weak donor-acceptor interaction.[46, 47] The exciplexes formed by **MQ**$^+$***** with alcohols of lower E_i may have a higher degree of charge-transfer character, which would justify their lower fluorescence efficiency. This is supported by the values of the radiative and nonradiative deactivation constants of the

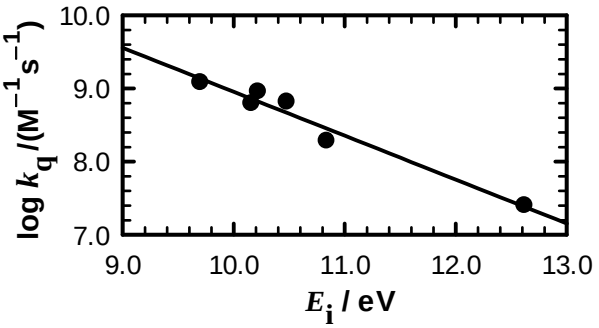

Fig. 4 Dependence of the quenching constant k_q on the ionization energy of the quenchers listed in Table 2.

exciplexes (Table 2): whereas k_r^E is almost constant for all exciplexes, a clear increase of k_{nr}^E is found for the quenchers with lower ionization energy. Nevertheless, the values of k_{nr}^E are sufficiently low to ascertain the weak charge transfer in the exciplexes even for the alcohols with stronger electron-donating capacity.

As we pointed out above, the main contribution to the quenching comes from the reaction of the exciplex with a second quencher molecule. The linear decrease of log k_q with increasing E_i of the quencher (Fig. 4) strongly supports the hypothesis that the process involves an electron transfer from the quencher to the exciplex. However, an explanation is required for the fact that 2,2,2- trifluoroethanol does not quench the **MQ**$^+$ fluorescence, despite having an intermediate E_i value between those of water and methanol (Table 2). Even the solvent acetonitrile has an E_i value (12.20 eV) lower than water,[42] but nevertheless, the fluorescence quantum yield of **MQ**$^+$ is higher in acetonitrile than in water (Table 1). What distinguishes 2,2,2-trifluoroethanol and acetonitrile from water and other alcohols are their different hydrogen-bond ability and acid–base character. This led us to think that, in addition to the electron transfer, a proton transfer may also have a role in the quenching process.

Quantum mechanical study of the MQ$^+$–2H$_2$O complex

In order to gain some insight into the quenching mechanism, we investigated by quantum mechanical methods the complex of **MQ**$^+$***** with two water molecules. We started by carrying out geometry optimizations for the **MQ**$^+$ molecule in the ground and in the first-excited electronic state. We used density functional theory (DFT and TD-DFT),[48, 49] together with the B3LYP functional[50, 51] and the correlation consistent polarized valence triple zeta basis set of Dunning *et al.* (cc-pVTZ)[52]. Taking the **MQ**$^+$ DFT(B3LYP)/cc-pVTZ geometry as starting point, we optimized the ground-state geometry of the complex that resulted from the addition of two water molecules. For this, we considered five initial intermolecular configurations with the two water molecules located at different positions, i.e. interacting with each other and also above and below the **MQ**$^+$ molecule ring plane. In the most stable configuration, the two water molecules were located on one side of the **MQ**$^+$ ion, with one of the water oxygen atoms on the plane of the **MQ**$^+$ rings and the second water molecule interacting with the first through a hydrogen bond. For this configuration, we optimized the ground- and the first-excited-state geometries using DFT and TD-DFT (B3LYP) and the cc-pVTZ and the aug-cc-pVTZ basis sets. The differences between the cc-pVTZ and the aug-cc-pVTZ intramolecular geometries were not significant, but this was not the case for the intermolecular parameters. Taking this into account, in the following we consider aug-cc-pVTZ results. The corresponding ground- and excited-state geometries are reported in the ESI† (Fig. 17S and Tables 1S and 2S, ESI†). The lowest excitation has a DFT(B3LYP)/aug-cc-pVTZ energy of 3.82 eV and the responsible orbitals are mainly the HOMO and the LUMO of the **MQ**$^+$ molecule.

The optimized excited-state geometry of the **MQ**$^+$*****–2H$_2$O complex (Fig. 5) shows a water dimer coordinated through an O atom to two H atoms of the quinolinium molecule. The main differences between the ground- and the excited-state geometries are due to the intermolecular interaction between the water dimer and the **MQ**$^+$ molecule. In the excitation, the water molecule that is closest to the **MQ**$^+$ unit suffers a displacement towards the closest hydrogen atom in the methyl group, and the distance between the two water molecules increases (the O–O distance varies from 2.801 Å to 2.822 Å). The distance between the water O and the methyl H (2.304 Å) is slightly larger than the distance between the O and the H atom of the quinolinium ring at position 2 (2.229 Å), and both are indicative of the existence of C–H···O hydrogen bonds.[53] The values of the exciplex formation equilibrium constant K are similar for water and alcohols (Table 2), indicating that the strength of the interaction of H$_2$O or ROH with **MQ**$^+$***** is about the same in all cases studied. This result is in accordance with the similar hydrogen-bond basicity of water and these alcohols,[54] so we presume the complexes of **MQ**$^+$***** with H$_2$O or ROH to have an analogous structure.

Proposal of a PCET quenching mechanism

We can take the structure of the complex formed by **MQ**$^+$***** with two water molecules in the gas phase as indicative of the more stable way of approaching the two water molecules to **MQ**$^+$***** in an aprotic solvent as acetonitrile. This structure is adequate for a PCET to take place. If this is true, electron transfer from the central water (or alcohol) molecule to **MQ**$^+$***** will occur in concert with proton transfer to the neighbouring water molecule through the pre-existing hydrogen bond. This is in agreement with the fact that the hypothetical radical cation intermediate of an initial electron transfer (ROH$^{\bullet+}$) is highly acidic,[55-57] and will transfer a proton to the second ROH molecule to form the more stable species RO$^\bullet$ and ROH$_2^+$. The feasibility of the concerted proton transfer would allow the electron transfer to occur by providing a lower-energy path to the reaction products.

The very low hydrogen-bond basicity of 2,2,2-trifluoroethanol[38, 39] would hinder the formation of the exciplex and the trimolecular reactive complex. Moreover, its

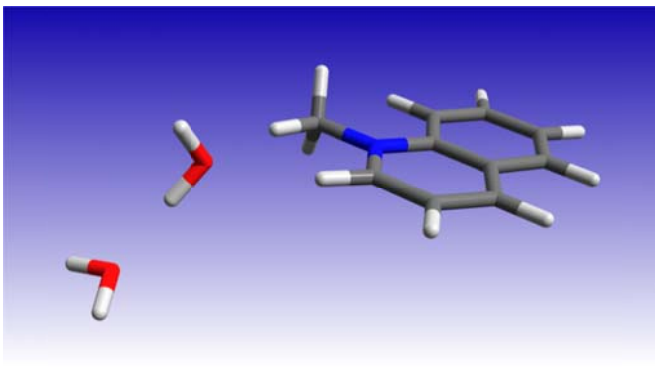

Fig. 5 B3LYP/aug-cc-pVTZ optimized geometry of the **MQ**$^+$*****–2H$_2$O complex in the first-excited singlet state.

proton basicity is also extremely low, as deduced from its very low gas basicity[58] and its inability to accept the proton of relatively strong photoacids in liquid solution.[59] These characteristics impede the PCET process for 2,2,2-trifluoroethanol. Acetonitrile has also a very low hydrogen-bond basicity and proton basicity in liquid solutions,[38, 39] and is unable to participate in a PCET reaction due to lack of ionisable protons. These facts explain why acetonitrile and 2,2,2-trifluoroethanol do not quench the fluorescence of the N-methylquinolinium cation, in spite of being more easily oxidized than water.

With the quenching constants obtained for methanol and ethanol solutions in acetonitrile (Table 2), we can calculate an extrapolated value of the fluorescence quantum yield of **MQ**$^+$ in pure alcohol solutions (24.70 mol dm^{-3} methanol and 17.13 mol dm^{-3} ethanol). The predicted values are $\Phi = 5.5 \times 10^{-3}$ for methanol and $\Phi = 6.2 \times 10^{-3}$ for ethanol. These results are in reasonable agreement with the experimental values (Table 1), taking into account the large extrapolation from dilute solutions and the change in the medium from acetonitrile to alcohol. Nevertheless, the fluorescence quantum yield of **MQ**$^+$ predicted in the same way for pure water solution ($\Phi = 1.1 \times 10^{-2}$) is much lower than the experimental value (Table 1). This led us to think that a change in the quenching mechanism must occur on increasing water concentration. To test this hypothesis, we measured the fluorescence intensities of **MQ**$^+$ in the whole concentration range from pure acetonitrile to pure water. The fluorescence spectral shape hardly changes for these mixtures (cf. Fig. 1 and Fig. 5S(C), ESI†), but the fluorescence intensity decreases with increasing water content until a molar fraction of $x_{H_2O} \approx 0.5$, increasing afterwards. Fig. 6 shows the influence of water content on the fluorescence intensity quotient F^0/F, with a maximum at equimolar amounts of water and acetonitrile.

The behaviour observed for **MQ**$^+$ in acetonitrile/water mixtures is probably due to the microheterogeneity of these solutions, which has been demonstrated by a range of different techniques.[60, 61] At low water concentrations, the water molecules form small aggregates of a few molecules, also associated with the acetonitrile molecules. As the water content is increased, microscopic domains of self-associated water exist, as well as acetonitrile domains, until the water content is so high that an extensive hydrogen-bonded network is established.[60] Our results (Fig. 6) point to the fact that the ability of the water molecules to cooperate via PCET to donate an electron is higher for small aggregates than for an extensive hydrogen-bonded network of water. This can be related to the higher ability of a water molecule that does not participate in the ordinary water structure to donate an electron pair toward a hydrogen bond than one that does.[61]

A close parallelism exists between the behaviour of **MQ**$^+$ here described and that of the stronger oxidant methyl viologen. The fluorescence of MV^{2+} is also quenched by water, methanol and ethanol, but not by acetonitrile or 2,2,2-trifluoroethanol.[45] Femtosecond transient absorption experiments in bulk methanol have shown that the radical cation of methyl viologen is produced at ultrafast rate (< 180 fs) as result of the oxidation of a solvent molecule by the photoexcited MV^{2+}.[45] To explain the rapid quenching of the first-excited singlet state of MV^{2+} in aqueous solution, Kohler and co-workers proposed a concerted proton–electron transfer reaction.[62] By using ultrafast spectroscopic techniques, they presented convincing evidence that the strongly oxidizing excited state of MV^{2+} triggers the proton-coupled oxidation of a water molecule, which transfers a proton to the bulk solvent and an electron to MV^{2+}* to form the hydroxyl radical. Although the $MV^{\bullet+}/OH^{\bullet}$ radical pair was not detected probably due to fast back electron transfer, a photoproduct was identified as the charge-transfer complex formed between ground-state MV^{2+} and a hydroxide ion. We propose here that a similar mechanism can take place for the weaker oxidant **MQ**$^+$* in acetonitrile solution, with a water or alcohol molecule in a H-bonded pair acting as efficient electron-donating entity towards **MQ**$^+$* through the concerted proton transfer to the second hydroxy molecule of the pair. This result is in accord with previous quantum-mechanical calculations, which show a strong decrease in E_i of water upon dimer formation.[63] The concerted action of a pair of water or alcohol molecules in proton transfer reactions has also been demonstrated.[64-67]

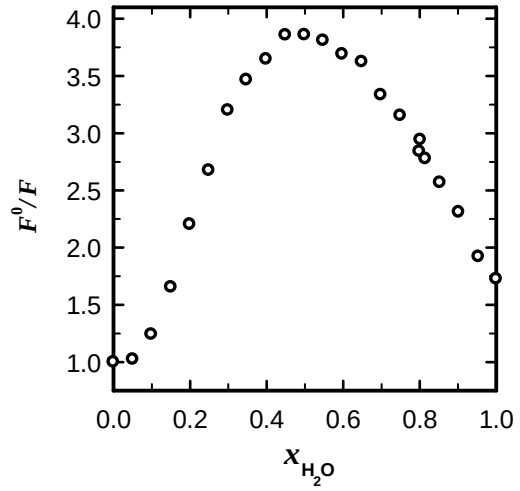

Fig. 6 Dependence of the relative fluorescence intensity of **MQ**$^+$ on the molar fraction of water in mixtures acetonitrile/water ($\tilde{\nu}_{exc}$ = 31650 cm^{-1}, $\tilde{\nu}_{em}$ = 24400 cm^{-1}).

Electron transfer from water or alcohols to other excited chromophores has also been established. Femtosecond experiments in bulk solvents showed that excited oxazine 750 is reduced by different aliphatic alcohols.[68] Moreover, several quantum-mechanical calculations on excited chromophores clustered with water or alcohols predict that an electron transfer from the hydroxy compound to the chromophore can take place. Examples comprise oxazine 750 clustered with two ethanol molecules[68] or 7H-adenine clustered with several water molecules.[69] In some cases, the initial electron transfer is followed by a proton transfer from water to the excited chromophore (for example, in the complexes pyridine-H_2O,[70] benzoquinone-H_2O,[71] 1-methylcytosine-$(H_2O)_2$,[72] 9H-adenine-$(H_2O)_5$[73] and acridine-H_2O).[74] The capacity of the triplet excited state of acridine orange to split the O–H bond of phenol

derivatives through PCET has also been experimentally demonstrated.[75]

According to our proposal, the quenching process of **MQ$^+$*** by small amounts of water and alcohols in acetonitrile solution can be described as a concerted multiple-site electron-proton transfer (MS-EPT),[22] also called bidirectional PCET,[18] in which the electron and proton transfers occur from a single donor (water or alcohol) to different acceptors. This type of PCET plays a major role in a variety of biological processes and in a wide range of chemical systems involving hydroxy compounds as electron and proton donors.[18, 22, 62, 76-81]

Recognition of the relatively high efficiency of water pairs as electron donors can contribute to understanding the puzzling photorelaxation and electron transfer mechanisms of biomolecules, where water molecules have been shown to play a fundamental role.[82, 83] Our results are also relevant to the issues of relaxation mechanisms of excited molecules in hydroxylic solvents, solar water splitting and solar fuel production.

Conclusions

The quantitative analysis of the fluorescence quenching of **MQ$^+$*** by small amounts of water and alcohols in acetonitrile solution revealed that upon excitation, emissive exciplexes are formed between **MQ$^+$*** and one molecule of water or alcohol. The fluorescence emission spectra of the exciplexes were resolved and their fluorescence efficiencies were determined. In all cases, the fluorescence of the exciplex was quenched by a second water or alcohol molecule, the quenching rate constant increasing as the ionization energy of the hydroxy compound decreased. We propose that this deactivation pathway is due to a photoinduced PCET involving an intermediate H-bonded complex of the excited quinolinium with a pair of molecules of the hydroxy compounds. In this pair, the electron transfer from H_2O/ROH to **MQ$^+$*** is facilitated by concerted proton transfer to the second molecule of the hydroxy compound. In accord with this mechanism, a very low basicity of the hydroxy compound inhibits the electron transfer. We also showed that an extensive hydrogen-bonded network of water molecules is less effective than the smaller aggregates for the enhancement of electron transfer via PCET.

Our findings support that water and alcohol dimers show a much stronger reducing power than the isolated molecules in an aprotic solvent. The results obtained may be relevant to the study of water oxidation and electron transfer in biological systems.

Conflicts of interest

There are no conflicts to declare.

Acknowledgements

This work has received financial support from Gobierno de España, Ministerio de Economía y Competitividad (Grant CTQ2014-59020-R), Xunta de Galicia (Grants ED431B 2016/024, ED431D R2016/007, ED431C 2017/17 and Centro Singular de Investigación de Galicia Accreditation 2016-2019, ED431G/09), and the European Union (European Regional Development Fund - ERDF). Fellowships from Conselho Nacional de Desenvolvimento Científico e Tecnológico (CNPq), Brasil (J.A.P.) and Xunta de Galicia, Spain (C.C.C.) are gratefully acknowledged. We thank Carlos Carreira Blanco for performing some fluorescence measurements.

References

1. N. A. Romero and D. A. Nicewicz, *Chem. Rev.*, 2016, **116**, 10075-10166.
2. T. Del Giacco, A. Faltoni and F. Elisei, *Phys. Chem. Chem. Phys.*, 2008, **10**, 200-210.
3. U. C. Yoon, S. L. Quillen, P. S. Mariano, R. Swanson, J. L. Stavinoha and E. Bay, *J. Am. Chem. Soc.*, 1983, **105**, 1204-1218.
4. S. Jayaraman and A. S. Verkman, *Biophys. Chem.*, 2000, **85**, 49-57.
5. C. D. Geddes, K. Apperson, J. Karolin and D. J. S. Birch, *Anal. Biochem.*, 2001, **293**, 60-66.
6. R. Rautela, P. Arora, N. K. Joshi, S. Pant and H. C. Joshi, *J. Mol. Liq.*, 2016, **218**, 632-636.
7. J. G. Harangozo, Z. Miskolczy, L. Biczok, V. Wintgens and C. Lorthioir, *J. Incl. Phenom. Macrocycl. Chem.*, 2015, **81**, 377-384.
8. Z. Miskolczy, J. G. Harangozo, L. Biczok, V. Wintgens, C. Lorthioir and C. Amiel, *Photochem. Photobiol. Sci.*, 2014, **13**, 499-508.
9. C. D. Geddes, *Meas. Sci. Technol.*, 2001, **12**, R53-R88.
10. C. D. Geddes, *Sensor Actuat. B-Chem.*, 2001, **72**, 188-195.
11. I. J. Bazany-Rodriguez, D. Martinez-Otero, J. Barroso-Flores, A. K. Yatsimirsky and A. Dorazco-Gonzalez, *Sensor Actuat. B-Chem.*, 2015, **221**, 1348-1355.
12. R. X. Zhang, P. F. Li, W. J. Zhang, N. Li and N. Zhao, *J. Mater. Chem. C*, 2016, **4**, 10479-10485.
13. S. C. Chao, J. Tretzel and F. W. Schneider, *J. Am. Chem. Soc.*, 1979, **101**, 134-139.
14. N. Mataga, H. Chosrowjan and S. Taniguchi, *J. Photochem. Photobiol. C*, 2005, **6**, 37-79.
15. Proton-Coupled Electron Transfer Themed Issue. *Chem. Rev. 2010, 110, 6937−7100.*
16. C. J. Gagliardi, B. C. Westlake, C. A. Kent, J. J. Paul, J. M. Papanikolas and T. J. Meyer, *Coord. Chem. Rev.*, 2010, **254**, 2459-2471.
17. S. Hammes-Schiffer, *J. Am. Chem. Soc.*, 2015, **137**, 8860-8871.
18. J. C. Lennox, D. A. Kurtz, T. Huang and J. L. Dempsey, *ACS Energy Lett.*, 2017, **2**, 1246-1256.
19. M. Hambourger, G. F. Moore, D. M. Kramer, D. Gust, A. L. Moore and T. A. Moore, *Chem. Soc. Rev.*, 2009, **38**, 25-35.
20. D. G. Nocera, *Acc. Chem. Res.*, 2012, **45**, 767-776.
21. S. Formosinho and M. Barroso, Eds, *Proton-coupled Electron Transfer: A Carrefour for Chemical Reactivity Traditions*, Royal Society of Chemistry, Cambridge, U.K., 2012.
22. D. R. Weinberg, C. J. Gagliardi, J. F. Hull, C. F. Murphy, C. A. Kent, B. C. Westlake, A. Paul, D. H. Ess, D. G. McCafferty and T. J. Meyer, *Chem. Rev.*, 2012, **112**, 4016-4093.
23. A. Migliore, N. F. Polizzi, M. J. Therien and D. N. Beratan, *Chem. Rev.*, 2014, **114**, 3381-3465.
24. Y. Zhang, X.-B. Li, A. M. Fleming, J. Dood, A. A. Beckstead, A. M. Orendt, C. J. Burrows and B. Kohler, *J. Am. Chem. Soc.*, 2016, **138**, 7395-7401.

25. Y. Zhang, K. de La Harpe, A. A. Beckstead, R. Improta and B. Kohler, *J. Am. Chem. Soc.*, 2015, **137**, 7059-7062.
26. O. S. Wenger, *Acc. Chem. Res.*, 2013, **46**, 1517-1526.
27. C. J. Gagliardi, L. Wang, P. Dongare, M. K. Brennaman, J. M. Papanikolas, T. J. Meyer and D. W. Thompson, *Proc. Natl. Acad. Sci. USA*, 2016, **113**, 11106-11109.
28. C. Costentin, M. Robert, J.-M. Saveant and C. Tard, *Acc. Chem. Res.*, 2014, **47**, 271-280.
29. J. J. Warren and J. M. Mayer, *Biochemistry*, 2015, **54**, 1863-1878.
30. J. Soetbeer, P. Dongare and L. Hammarström, *Chem. Sci.*, 2016, **7**, 4607-4612.
31. B. H. Solis, A. G. Maher, D. K. Dogutan, D. G. Nocera and S. Hammes-Schiffer, *Proc. Natl. Acad. Sci. U. S. A.*, 2016, **113**, 485-492.
32. G. A. Crosby and J. N. Demas, *J. Phys. Chem.*, 1971, **75**, 991-1024.
33. W. H. Melhuish, *J. Phys. Chem.*, 1961, **65**, 229-235.
34. D. Siano, B. and D. Metzler, E., *J. Chem. Phys.*, 1969, **51**, 1856-1861.
35. D. W. Marquardt, *J. Soc. Ind. Appl. Math.*, 1963, **11**, 431-441.
36. Joint Committee for Guides in Metrology (JCGM), *Evaluation of Measurement Data - Guide to the Expression of Uncertainty in Measurement*, JCGM, Paris, 2008.
37. M. J. Frisch, G. W. Trucks, H. B. Schlegel, G. E. Scuseria, M. A. Robb, J. R. Cheeseman, G. Scalmani, V. Barone, B. Mennucci, G. A. Petersson, H. Nakatsuji, M. Caricato, X. Li, H. P. Hratchian, A. F. Izmaylov, J. Bloino, G. Zheng, J. L. Sonnenberg, M. Hada, M. Ehara, K. Toyota, R. Fukuda, J. Hasegawa, M. Ishida, T. Nakajima, Y. Honda, O. Kitao, H. Nakai, T. Vreven, J. A. Montgomery Jr., J. E. Peralta, F. Ogliaro, M. J. Bearpark, J. Heyd, E. N. Brothers, K. N. Kudin, V. N. Staroverov, R. Kobayashi, J. Normand, K. Raghavachari, A. P. Rendell, J. C. Burant, S. S. Iyengar, J. Tomasi, M. Cossi, N. Rega, N. J. Millam, M. Klene, J. E. Knox, J. B. Cross, V. Bakken, C. Adamo, J. Jaramillo, R. Gomperts, R. E. Stratmann, O. Yazyev, A. J. Austin, R. Cammi, C. Pomelli, J. W. Ochterski, R. L. Martin, K. Morokuma, V. G. Zakrzewski, G. A. Voth, P. Salvador, J. J. Dannenberg, S. Dapprich, A. D. Daniels, Ö. Farkas, J. B. Foresman, J. V. Ortiz, J. Cioslowski and D. J. Fox, *Gaussian 09, Revision A.02*, Gaussian, Inc., Wallingford, CT, USA, 2009.
38. C. Laurence, K. A. Brameld, J. Graton, J.-Y. Le Questel and E. Renault, *J. Med. Chem.*, 2009, **52**, 4073-4086.
39. C. Laurence, J. Legros, P. Nicolet, D. Vuluga, A. Chantzis and D. Jacquemin, *J. Phys. Chem. B*, 2014, **118**, 7594-7608.
40. W. Al-Soufi, M. Novo and M. Mosquera, *Appl. Spectrosc.*, 2001, **55**, 630-636.
41. W. Al-Soufi, M. Novo, M. Mosquera and F. Rodríguez Prieto, in *Reviews in Fluorescence 2009*, ed. C. D. Geddes, Springer, New York, 2011, pp. 23-45.
42. S. G. Lias, J. E. Bartmess, J. F. Liebman, J. L. Holmes, R. D. Levin and W. G. Mallard, in *NIST Chemistry WebBook, NIST Standard Reference Database Number 69*, eds. P. J. Linstrom and W. G. Mallard, National Institute of Standards and Technology, Gaithersburg MD, 20899, http://webbook.nist.gov, (retrieved November 16, 2017).
43. J. M. Fossey, P.; Thissen, R.; Audier, H. E., *Int. J. Mass Spectrom.*, 2003, **227**, 373-380.
44. Y. Fu, L. Liu, H. Z. Yu, Y. M. Wang and Q. X. Guo, *J. Am. Chem. Soc.*, 2005, **127**, 7227-7234.
45. J. Peon, X. Tan, J. D. Hoerner, C. G. Xia, Y. F. Luk and B. Kohler, *J. Phys. Chem. A*, 2001, **105**, 5768-5777.
46. A. Rosspeintner and E. Vauthey, *Phys. Chem. Chem. Phys.*, 2014, **16**, 25741-25754.
47. B. Dereka, M. Koch and E. Vauthey, *Acc. Chem. Res.*, 2017, **50**, 426-434.
48. P. Hohenberg and W. Kohn, *Phys. Rev. B*, 1964, **136**, B864.
49. W. Kohn and L. J. Sham, *Phys. Rev.*, 1965, **140**, A1133-A1138.
50. A. D. Becke, *J. Chem. Phys.*, 1993, **98**, 5648-5652.
51. C. T. Lee, W. T. Yang and R. G. Parr, *Phys. Rev. B*, 1988, **37**, 785-789.
52. T. H. Dunning, *J. Chem. Phys.*, 1989, **90**, 1007-1023.
53. G. Gilli and P. Gilli, *The Nature of the Hydrogen Bond : Outline of a Comprehensive Hydrogen Bond Theory*, Oxford University Press, Oxford, U. K., 2013.
54. C. Laurence, M. Berthelot, M. Helbert and K. Sraidi, *J. Phys. Chem.*, 1989, **93**, 3799-3802.
55. R. G. Pearson, *J. Am. Chem. Soc.*, 1986, **108**, 6109-6114.
56. F. G. Bordwell and J. P. Cheng, *J. Am. Chem. Soc.*, 1989, **111**, 1792-1795.
57. X. Cai, M. Sakamoto, M. Fujitsuka and T. Majima, *J. Phys. Chem. A*, 2007, **111**, 1788-1791.
58. E. P. L. Hunter and S. G. Lias, *J. Phys. Chem. Ref. Data*, 1998, **27**, 413-656.
59. A. Brenlla, M. Veiga Gutierrez, M. C. Rios Rodriguez, F. Rodriguez-Prieto, M. Mosquera and J. L. Perez Lustres, *J. Phys. Chem. Lett.*, 2014, **5**, 989-994.
60. Y. Marcus, *J. Phys. Org. Chem.*, 2012, **25**, 1072-1085.
61. Y. Marcus and Y. Migron, *J. Phys. Chem.*, 1991, **95**, 400-406.
62. J. D. Henrich, S. Suchyta and B. Kohler, *J. Phys. Chem. B*, 2015, **119**, 2737-2748.
63. J. Segarra-Martí, M. Merchán and D. Roca-Sanjuán, *J. Chem. Phys.*, 2012, **136**, 244306.
64. M. C. Ríos Rodríguez, J. C. Penedo, R. J. Willemse, M. Mosquera and F. Rodríguez-Prieto, *J. Phys. Chem. A*, 1999, **103**, 7236-7243.
65. J. C. Penedo, M. Mosquera and F. Rodríguez-Prieto, *J. Phys. Chem. A*, 2000, **104**, 7429-7441.
66. S.-Y. Park, T. G. Kim, M. J. Ajitha, K. Kwac, Y. M. Lee, H. Kim, Y. Jung and O.-H. Kwon, *Phys. Chem. Chem. Phys.*, 2016, **18**, 24880-24889.
67. W. Siebrand, Z. Smedarchina, E. Martínez-Núñez and A. Fernández-Ramos, *Phys. Chem. Chem. Phys.*, 2016, **18**, 22712-22718.
68. G.-J. Zhao, J.-Y. Liu, L.-C. Zhou and K.-L. Han, *J. Phys. Chem. B*, 2007, **111**, 8940-8945.
69. M. Barbatti, *J. Am. Chem. Soc.*, 2014, **136**, 10246-10249.
70. X. Liu, A. L. Sobolewski, R. Borrelli and W. Domcke, *Phys. Chem. Chem. Phys.*, 2013, **15**, 5957-5966.
71. T. N. V. Karsili, D. Tuna, J. Ehrmaier and W. Domcke, *Phys. Chem. Chem. Phys.*, 2015, **17**, 32183-32193.
72. R. Szabla, H. Kruse, J. Sponer and R. W. Gora, *Phys. Chem. Chem. Phys.*, 2017, **19**, 17531-17537.
73. X. Wu, T. N. V. Karsili and W. Domcke, *ChemPhysChem*, 2016, **17**, 1298-1304.
74. X. Liu, T. N. V. Karsili, A. L. Sobolewski and W. Domcke, *J. Phys. Chem. B*, 2015, **119**, 10664-10672.
75. T. T. Eisenhart and J. L. Dempsey, *J. Am. Chem. Soc.*, 2014, **136**, 12221-12224.
76. L. Biczok, N. Gupta and H. Linschitz, *J. Am. Chem. Soc.*, 1997, **119**, 12601-12609.
77. L. Biczok, T. Berces and H. Linschitz, *J. Am. Chem. Soc.*, 1997, **119**, 11071-11077.
78. A. A. Pizano, J. L. Yang and D. G. Nocera, *Chem. Sci.*, 2012, **3**, 2457-2461.

79. J. Chen, M. Kuss-Petermann and O. S. Wenger, *J. Phys. Chem. B*, 2015, **119**, 2263-2273.
80. M.-T. Zhang, J. Nilsson and L. Hammarström, *Energy Environ. Sci.*, 2012, **5**, 7732-7736.
81. W. D. Morris and J. M. Mayer, *J. Am. Chem. Soc.*, 2017, **139**, 10312-10319.
82. I. M. C. van Amsterdam, M. Ubbink, O. Einsle, A. Messerschmidt, A. Merli, D. Cavazzini, G. L. Rossi and G. W. Canters, *Nat. Struct.Biol.*, 2002, **9**, 48-52.
83. P. Ball, *Chem. Rev.*, 2008, **108**, 74-108.

Table of contents

The proposed mechanism involves an electron transfer from H_2O/ROH to the excited quinolinium, concerted with proton transfer to the second hydroxy molecule.

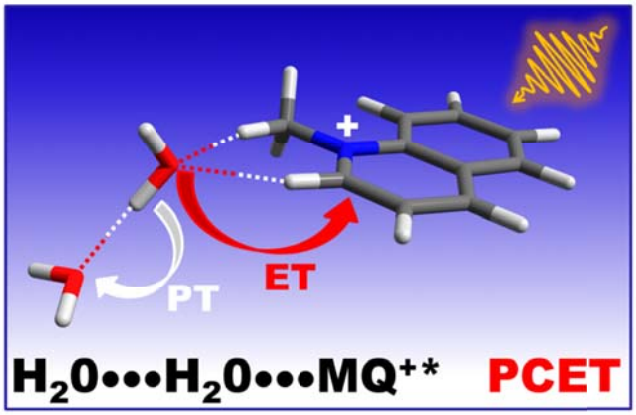

Electronic Supplementary Information

Fluorescence Quenching of the N-Methylquinolinium Cation by Pairs of Water or Alcohol Molecules

Flor Rodríguez-Prieto, Carlos Costa Corbelle, Berta Fernández, Jorge A. Pedro, M. Carmen Ríos Rodríguez* and Manuel Mosquera**

Centro Singular de Investigación en Química Biolóxica e Materiais Moleculares (CIQUS) and Departamento de Química Física, Facultade de Química, Universidade de Santiago de Compostela, E-15782 Santiago de Compostela, Spain.

Contents

Page

Title page and contents…… S1
Kinetic model……..……..…….. S2
Figure 1S. Absorption and fluorescence spectra of **MQ^+** in water…….…….. S5
Figure 2S. Absorption and fluorescence spectra of **MQ^+** in methanol...…….. S5
Figure 3S. Absorption and fluorescence spectra of **MQ^+** in ethanol.……..……. S6
Figure 4S. Fluorescence spectra of **MQ^+** in acetonitrile, water, methanol and ethanol…..……. S6
Figure 5S. Influence of water on the fluorescence of **MQ^+** in acetonitrile.……..…… S7
Figure 6S. Influence of ethanol on the fluorescence of **MQ^+** in acetonitrile.…….…….…..... S8
Figure 7S. Influence of 1-propanol on the fluorescence of **MQ^+** in acetonitrile……...……. S9
Figure 8S. Influence of 1,2-ethanediol on the fluorescence of **MQ^+** in acetonitrile..…….……. S10
Figure 9S. Influence of 1,3-propanediol on the fluorescence of **MQ^+** in acetonitrile.……..... S11
Figure 10S. Fluorescence of **MQ^+** in acetonitrile with addition of 2,2,2-trifluoroethanol…..... S12
Figure 11S. Fluorescence decay of **MQ^+** in acetonitrile with addition of alcohols..…..…..…… S12
Figure 12S. PCGA results of the fluorescence of **MQ^+** in acetonitrile with water.……. S13
Figure 13S. PCGA results of the fluorescence of **MQ^+** in acetonitrile with ethanol.…….. S14
Figure 14S. PCGA results of the fluorescence of **MQ^+** in acetonitrile with 1-propanol.…..…… S15
Figure 15S. PCGA results of the fluorescence of **MQ^+** in acetonitrile with 1,2-ethanediol..... S16
Figure 16S. PCGA results of the fluorescence of **MQ^+** in acetonitrile with 1,3-propanediol……. S17
Figure 17S. Atom numbering for the complex **MQ^+–$2H_2O$**.…….……..…… S18
Table 1S. Atomic coordinates for the optimized geometry of **MQ^+–$2H_2O$** in the ground state…….. S19
Table 2S. Atomic coordinates for the optimized geometry of **MQ^+–$2H_2O$** in the excited state…….. S20

Kinetic model

From Scheme 1, the exciplex formation equilibrium constant *K* and the excited-state concentrations of **MQ^{+}*** and **E*** are given by eqs S1 to S3, where $[T^*]$ is the total concentration of excited species (eq S4).

$$K = \frac{[E^*]}{[MQ^{+*}]\,[ROH]} \tag{S1}$$

$$[MQ^{+*}] = \frac{[T^*]}{1 + K\,[ROH]} \tag{S2}$$

$$[E^*] = \frac{K\,[ROH][T^*]}{1 + K\,[ROH]} \tag{S3}$$

$$[T^*] = [MQ^{+*}] + [E^*] \tag{S4}$$

The time dependence of [T*] after a short light pulse is given by:

$$-\frac{d[T^*]}{dt} = k_{MQ}\,[MQ^{+*}] + (k_E + k_q\,[ROH])\,[E^*] \tag{S5}$$

Integration of eq S5, together with eqs S2 and S3, leads to relations S6 and S7, where $[T^*]_0$ is the initial concentration of excited species.

$$[T^*] = [T^*]_0 e^{-k\,t} \tag{S6}$$

$$k = \tau^{-1} = \frac{k_{MQ} + K\,k_E\,[ROH] + K\,k_q\,[ROH]^2}{1 + K\,[ROH]} \tag{S7}$$

In the absence of quenchers, $\tau^0 = 1/k_{MQ}$, and therefore:

$$\frac{\tau^0}{\tau} = \frac{1 + \frac{K\,k_E}{k_{MQ}}\,[ROH] + \frac{K\,k_q}{k_{MQ}}\,[ROH]^2}{1 + K\,[ROH]} \tag{S8}$$

From eqs S6, S2, and S3, the time dependence of [**MQ**$^{+}$*****] and [**E***] can be easily calculated. Both show, like [**T***], a monoexponential decay with rate constant *k*, which displays a complex dependence on the hydroxy compound concentration (eq S7).

The fluorescence spectra of **MQ**$^{+}$***** and **E*** (vectors $\boldsymbol{F}_{\mathbf{MQ}}$ and $\boldsymbol{F}_{\mathbf{E}}$) depend on the steady-state (ss) concentrations of these species and are given by relations S9 and S10:

$$\boldsymbol{F}_{\mathbf{MQ}} = \chi^{\mathbf{MQ}}\, k_r^{\mathrm{MQ}} \left[\mathrm{MQ}^{+*}\right]_{\mathrm{ss}} \tag{S9}$$

$$\boldsymbol{F}_{\mathbf{E}} = \chi^{\mathbf{E}}\, k_r^{\mathrm{E}} \left[\mathrm{E}^{*}\right]_{\mathrm{ss}} \tag{S10}$$

In these equations, k_r^{MQ} and k_r^{E} are the radiative deactivation constants of **MQ**$^{+}$***** and **E***, and the vectors $\boldsymbol{\chi}^{\mathbf{MQ}}$ and $\boldsymbol{\chi}^{\mathbf{E}}$ are the fluorescence emission spectra of **MQ**$^{+}$***** and **E***with the area normalized to unity, multiplied by a common instrumental factor. $[MQ^{+*}]_{ss}$ and $[E^{*}]_{ss}$ are the steady-state concentrations of the respective species, obtained under continuous illumination.

Integration of eq S6 between time 0 and ∞ gives the steady-state concentration of the excited species, $[T^{*}]_{ss}$. Substitution of $[T^{*}]_{ss}$ into eqs S2 and S3 gives the steady-state concentrations $[MQ^{+*}]_{ss}$ and $[E^{*}]_{ss}$, which substituted into eqs S9 and S10, yield:

$$\boldsymbol{F}_{\mathbf{MQ}} = \chi^{\mathbf{MQ}}\, \frac{k_r^{\mathrm{MQ}}}{k_{\mathrm{MQ}}} \left[\mathrm{T}^{*}\right]_0 \frac{1}{1 + \frac{K\,k_{\mathrm{E}}}{k_{\mathrm{MQ}}}[\mathrm{ROH}] + \frac{K\,k_{\mathrm{q}}}{k_{\mathrm{MQ}}}[\mathrm{ROH}]^2} \tag{S11}$$

$$\boldsymbol{F}_{\mathbf{E}} = \chi^{\mathbf{E}}\, \frac{k_r^{\mathrm{E}}}{k_{\mathrm{E}}} \left[\mathrm{T}^{*}\right]_0 \frac{\frac{K\,k_{\mathrm{E}}}{k_{\mathrm{MQ}}}[\mathrm{ROH}]}{1 + \frac{K\,k_{\mathrm{E}}}{k_{\mathrm{MQ}}}[\mathrm{ROH}] + \frac{K\,k_{\mathrm{q}}}{k_{\mathrm{MQ}}}[\mathrm{ROH}]^2} \tag{S12}$$

The first factors of eqs S11 and S12 define $\boldsymbol{F}_{\mathbf{MQ}}^{\mathbf{0}}$ and $\boldsymbol{F}_{\mathbf{E}}^{\mathbf{0}}$, the fluorescence spectra that would be obtained for **MQ**$^{+}$***** and **E*** if each absorbed photon formed an excited molecule of the respective species and only the unimolecular deactivation of these species would be operative:

$$\boldsymbol{F}_{\mathbf{MQ}}^{\mathbf{0}} = \chi^{\mathbf{MQ}}\, \frac{k_r^{\mathrm{MQ}}}{k_{\mathrm{MQ}}} \left[\mathrm{T}^{*}\right]_0 \tag{S13}$$

$$\boldsymbol{F}_{\mathbf{E}}^{\mathbf{0}} = \chi^{\mathrm{E}} \frac{k_r^{\mathrm{E}}}{k_{\mathrm{E}}} \left[\mathrm{T}^*\right]_0 \tag{S14}$$

The observed fluorescence spectrum is therefore:

$$\boldsymbol{F} = \boldsymbol{F}_{\mathbf{MQ}} + \boldsymbol{F}_{\mathbf{E}} = C_{\mathrm{MQ}} \boldsymbol{F}_{\mathbf{MQ}}^{\mathbf{0}} + C_{\mathrm{E}} \boldsymbol{F}_{\mathbf{E}}^{\mathbf{0}} \tag{S15}$$

where the coefficients C_{MQ} and C_{E}, which represent the contributions of $\mathbf{MQ}^{+}\mathbf{*}$ and $\mathbf{E}^{*}$ spectra to the experimental spectrum, are given by:

$$C_{\mathrm{MQ}} = \frac{1}{1 + \frac{K\,k_{\mathrm{E}}}{k_{\mathrm{MQ}}}[\mathrm{ROH}] + \frac{K\,k_q}{k_{\mathrm{MQ}}}[\mathrm{ROH}]^2} \tag{S16}$$

$$C_{\mathrm{E}} = \frac{\frac{K\,k_{\mathrm{E}}}{k_{\mathrm{MQ}}}[\mathrm{ROH}]}{1 + \frac{K\,k_{\mathrm{E}}}{k_{\mathrm{MQ}}}[\mathrm{ROH}] + \frac{K\,k_{\mathrm{q}}}{k_{\mathrm{MQ}}}[\mathrm{ROH}]^2} \tag{S17}$$

We denote by Φ_{MQ}^{0} the fluorescence quantum yield of $\mathbf{MQ}^{+}$ in ACN in the absence of quenchers ($\Phi_{\mathrm{MQ}}^{0} = k_r^{\mathrm{MQ}}/k_{\mathrm{MQ}}$) and by η_{E}^{0} the fluorescence quantum efficiency of $\mathbf{E}^{*}$ if only the unimolecular photophysical deactivation of this excited species would be operative ($\eta_{\mathrm{E}}^{0} = k_r^{\mathrm{E}}/k_{\mathrm{E}}$). As $\boldsymbol{F}_{\mathbf{MQ}}^{\mathbf{0}}$ and $\boldsymbol{F}_{\mathbf{E}}^{\mathbf{0}}$ are normalized to the same concentration of excited species (eqs S13 and S14), the ratio of their integrated areas equals the ratio of fluorescence quantum yields:

$$\frac{\int \boldsymbol{F}_{\mathbf{MQ}}^{\mathbf{0}} \mathrm{d}\tilde{\nu}}{\int \boldsymbol{F}_{\mathbf{E}}^{\mathbf{0}} \mathrm{d}\tilde{\nu}} = \frac{\Phi_{\mathrm{MQ}}^{0}}{\eta_{\mathrm{E}}^{0}} \tag{S18}$$

From the experimental value of this ratio and the known value of Φ_{MQ}^{0}, we calculate η_{E}^{0}, which together with k_{E} allows the determination of the radiative and nonradiative deactivation constant of the exciplex:

$$k_r^{\mathrm{E}} = \eta_{\mathrm{E}}^{0} k_{\mathrm{E}} \tag{S19}$$

$$k_{nr}^{\mathrm{E}} = k_{\mathrm{E}} - k_r^{\mathrm{E}} \tag{S20}$$

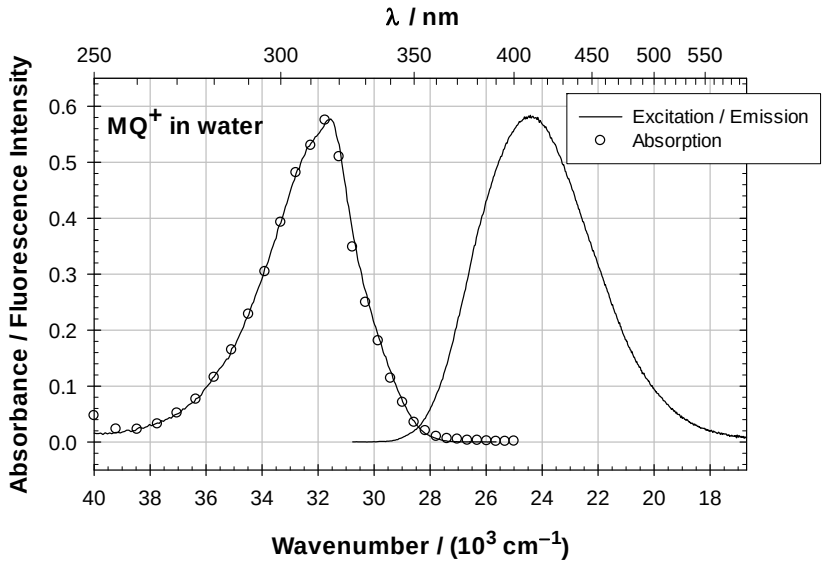

Figure 1S. Normalized absorption, fluorescence excitation, and fluorescence emission spectra of the N-methylquinolinium cation in water. [$\mathbf{MQ}^+$] = 9.29×10^{-6} M (fluorescence spectra) and [$\mathbf{MQ}^+$] = 7.65×10^{-5} M (absorption spectrum). $\tilde{\nu}_{excitation}$ = 31950 cm^{-1}. $\tilde{\nu}_{emission}$ = 24630 cm^{-1}.

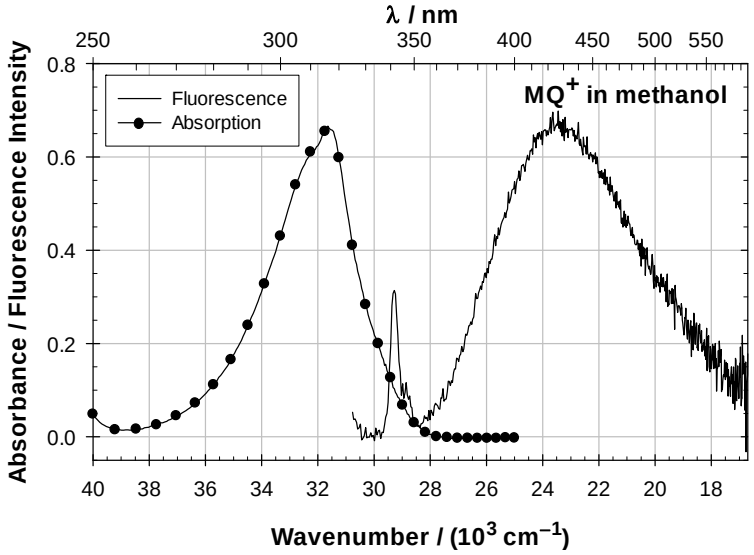

Figure 2S. Normalized absorption and fluorescence emission spectra of the N-methyl-quinolinium cation in methanol, and solvent Raman band. [$\mathbf{MQ}^+$] = 9.03×10^{-6} M (fluorescence spectrum) and [$\mathbf{MQ}^+$] = 8.45×10^{-5} M (absorption spectrum). $\tilde{\nu}_{excitation}$ = 31950 cm^{-1}.

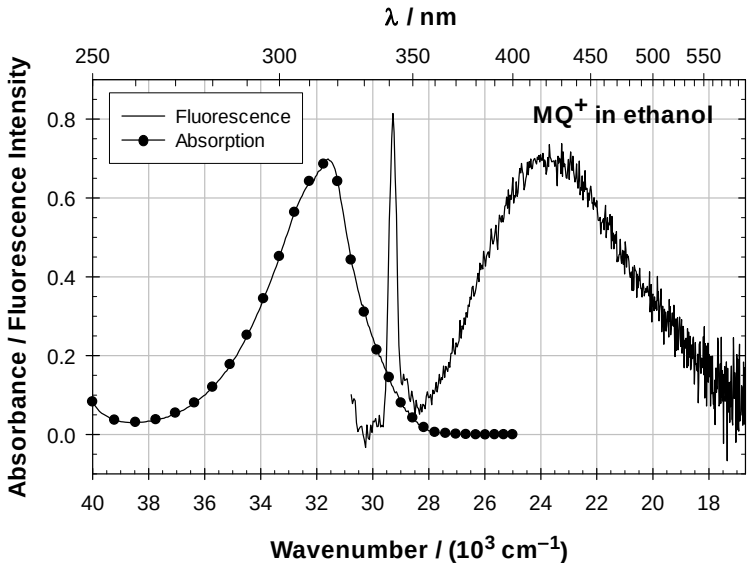

Figure 3S. Normalized absorption and fluorescence emission spectra of the N-methyl-quinolinium cation in ethanol, and solvent Raman band. [$\mathbf{MQ}^+$] = 9.86 × 10^{-6} M (fluorescence spectrum) and [$\mathbf{MQ}^+$] = 9.23 × 10^{-5} M (absorption spectrum). $\tilde{\nu}_{excitation}$ = 31950 cm^{-1}.

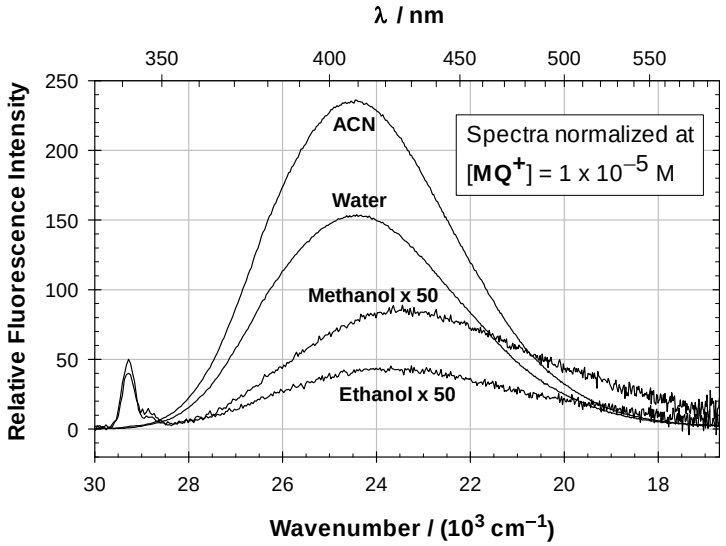

Figure 4S. Fluorescence emission spectra of the N-methylquinolinium cation in acetonitrile, water, methanol and ethanol, normalized at $\mathbf{MQ}^+$ concentration of 1 × 10^{-5} M, and alcohol Raman band. The intensity of the spectra in methanol and ethanol were multiplied by a factor of 50. $\tilde{\nu}_{excitation}$ = 31950 cm^{-1}.

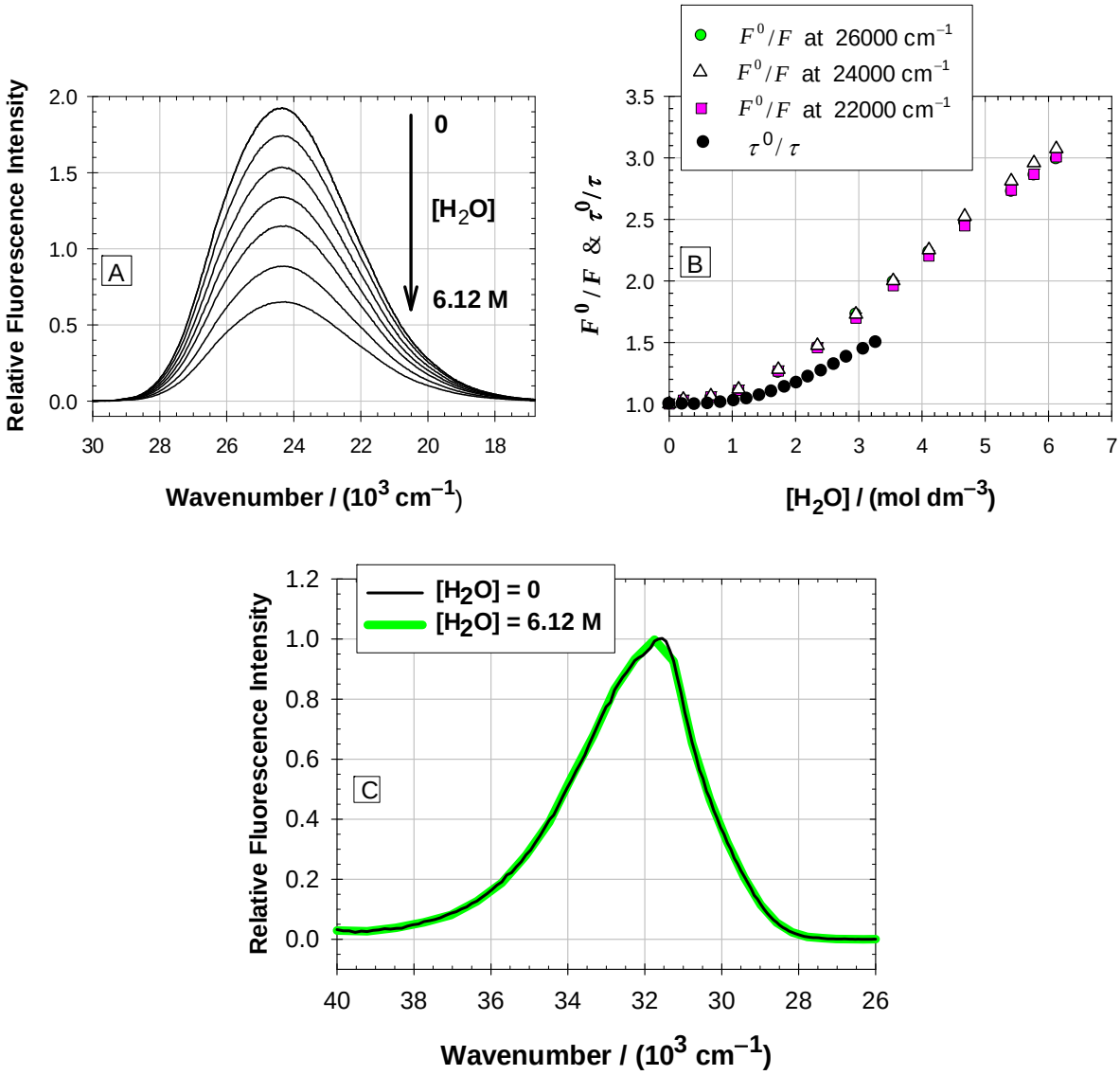

Figure 5S. Influence of water on the fluorescence spectra of $\mathbf{MQ^+}$ in acetonitrile: (A) Fluorescence emission spectra with increasing concentration of water in the range 0 to 6.12 mol/dm^3 ($\tilde{\nu}_{\mathbf{exc}}$ = 31950 cm^{-1}); (B) Influence of water concentration on the fluorescence intensity ratio F^0/F at various emission wavenumbers ($\tilde{\nu}_{\mathbf{exc}}$ = 31950 cm^{-1}), and on the fluorescence lifetime ratio τ^0/τ ($\tilde{\nu}_{\mathbf{exc}}$ = 32450 cm^{-1}, $\tilde{\nu}_{\mathbf{em}}$ = 24400 cm^{-1}); (C) Normalized fluorescence excitation spectra in pure acetonitrile and with addition of 6.12 mol/dm^3 of water ($\tilde{\nu}_{\mathbf{em}}$ = 24630 cm^{-1}). [$\mathbf{MQ^+}$] = 9.13 × 10^{-6} mol/dm^3 for the steady-state measurements and 1.04 × 10^{-4} mol/dm^3 for the lifetime measurements.

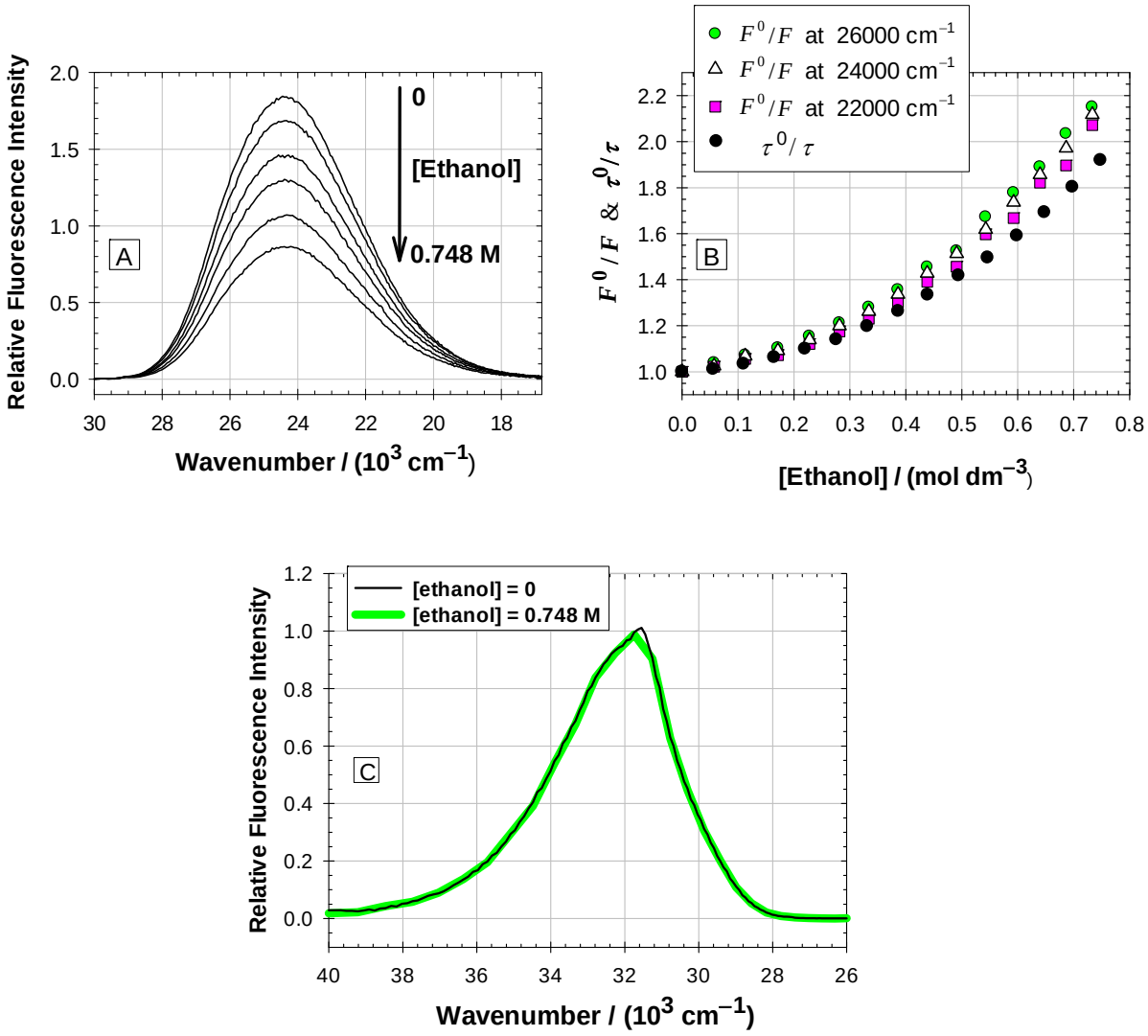

Figure 6S. Influence of ethanol on the fluorescence spectra of $\mathbf{MQ^+}$ in acetonitrile: (A) Fluorescence emission spectra with increasing concentration of ethanol in the range 0 to 0.748 mol/dm^3 ($\tilde{\nu}_{\mathbf{exc}}$ = 31950 cm^{-1}); (B) Influence of ethanol concentration on the fluorescence intensity ratio F^0/F at various emission wavenumbers ($\tilde{\nu}_{\mathbf{exc}}$ = 31950 cm^{-1}), and on the fluorescence lifetime ratio τ^0/τ ($\tilde{\nu}_{\mathbf{exc}}$ = 32450 cm^{-1}, $\tilde{\nu}_{\mathbf{em}}$ = 24400 cm^{-1}); (C) Normalized fluorescence excitation spectra in pure acetonitrile and with addition of 0.748 mol/dm^3 of ethanol ($\tilde{\nu}_{\mathbf{em}}$ = 24630 cm^{-1}). [$\mathbf{MQ^+}$] = 8.25 × 10^{-6} mol/dm^3 for the steady-state measurements and 1.02 × 10^{-4} mol/dm^3 for the lifetime measurements.

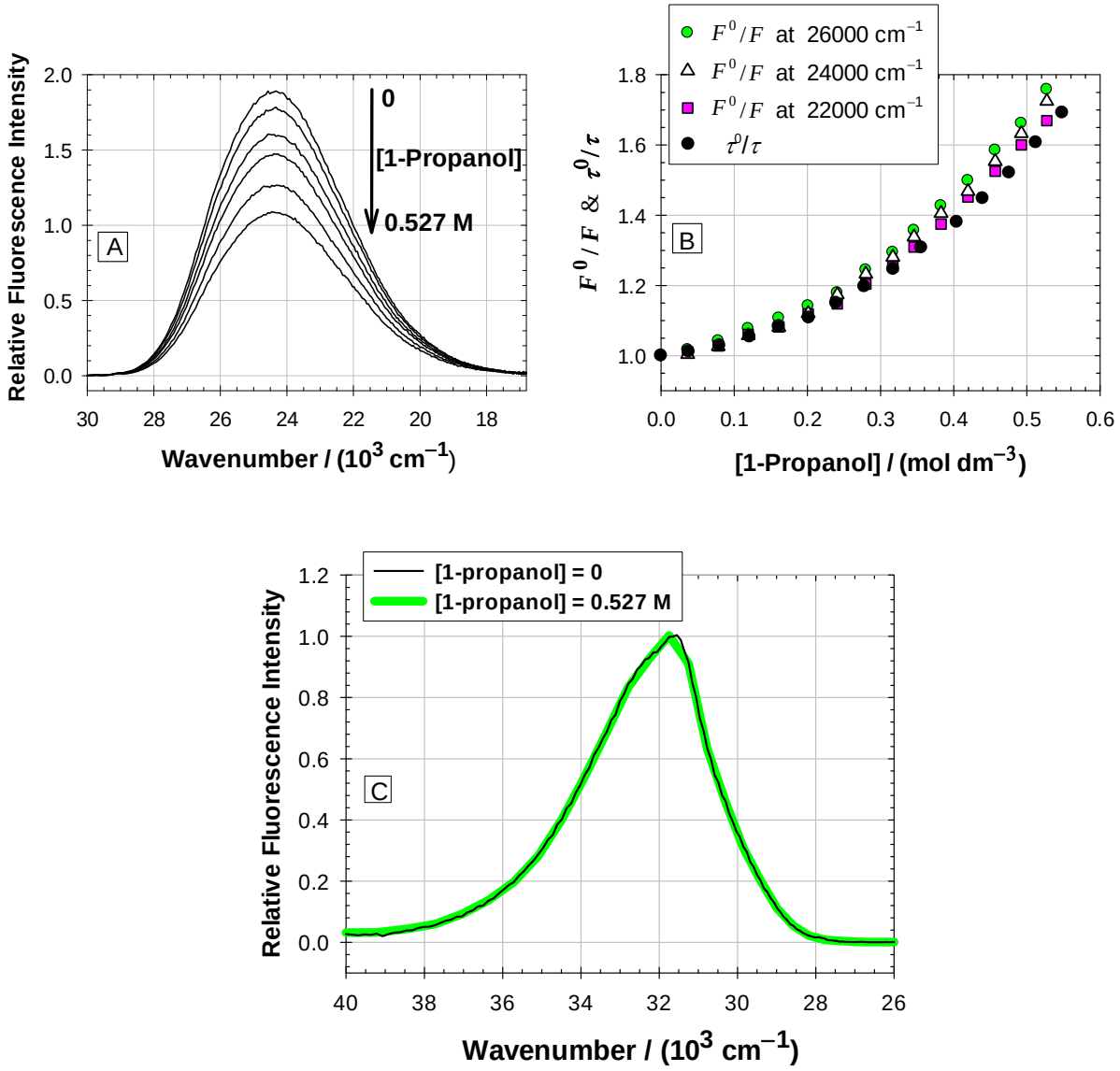

Figure 7S. Influence of 1-propanol on the fluorescence spectra of $\mathbf{MQ^+}$ in acetonitrile: (A) Fluorescence emission spectra with increasing concentration of 1-propanol in the range 0 to 0.527 mol/dm^3 ($\tilde{\nu}_{\mathbf{exc}}$ = 31950 cm^{-1}); (B) Influence of 1-propanol concentration on the fluorescence intensity ratio F^0/F at various emission wavenumbers ($\tilde{\nu}_{\mathbf{exc}}$ = 31950 cm^{-1}), and on the fluorescence lifetime ratio τ^0/τ ($\tilde{\nu}_{\mathbf{exc}}$ = 32450 cm^{-1}, $\tilde{\nu}_{\mathbf{em}}$ = 24400 cm^{-1}); (C) Normalized fluorescence excitation spectra in pure acetonitrile and with addition of 0.527 mol/dm^3 of 1-propanol ($\tilde{\nu}_{\mathbf{em}}$ = 24630 cm^{-1}). [$\mathbf{MQ^+}$] = 8.95 × 10^{-6} mol/dm^3 for the steady-state measurements and 1.00 × 10^{-4} mol/dm^3 for the lifetime measurements.

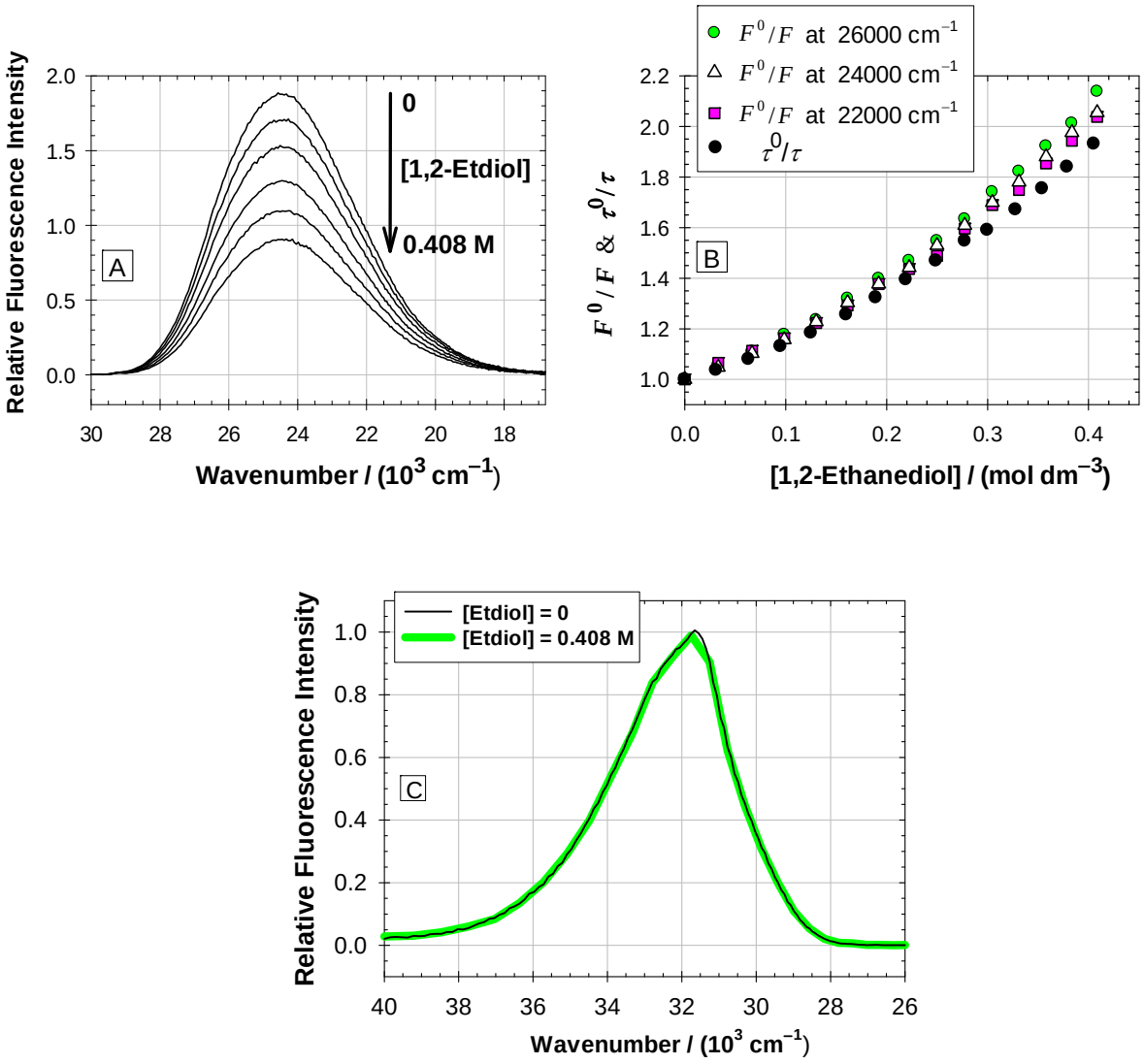

Figure 8S. Influence of 1,2-ethanediol on the fluorescence spectra of $\mathbf{MQ^+}$ in acetonitrile: (A) Fluorescence emission spectra with increasing concentration of 1,2-ethanediol in the range 0 to 0.408 mol/dm^3 ($\tilde{\nu}_{\mathbf{exc}}$ = 31950 cm^{-1}); (B) Influence of 1,2-ethanediol concentration on the fluorescence intensity ratio F^0/F at various emission wavenumbers ($\tilde{\nu}_{\mathbf{exc}}$ = 31950 cm^{-1}), and on the fluorescence lifetime ratio τ^0/τ ($\tilde{\nu}_{\mathbf{exc}}$ = 32450 cm^{-1}, $\tilde{\nu}_{\mathbf{em}}$ = 24400 cm^{-1}); (C) Normalized fluorescence excitation spectra in pure acetonitrile and with addition of 0.408 mol/dm^3 of 1,2-ethanediol ($\tilde{\nu}_{\mathbf{em}}$ = 24630 cm^{-1}). [$\mathbf{MQ^+}$] = 8.27 × 10^{-6} mol/dm^3 for the steady-state measurements and 9.95 × 10^{-5} mol/dm^3 for the lifetime measurements.

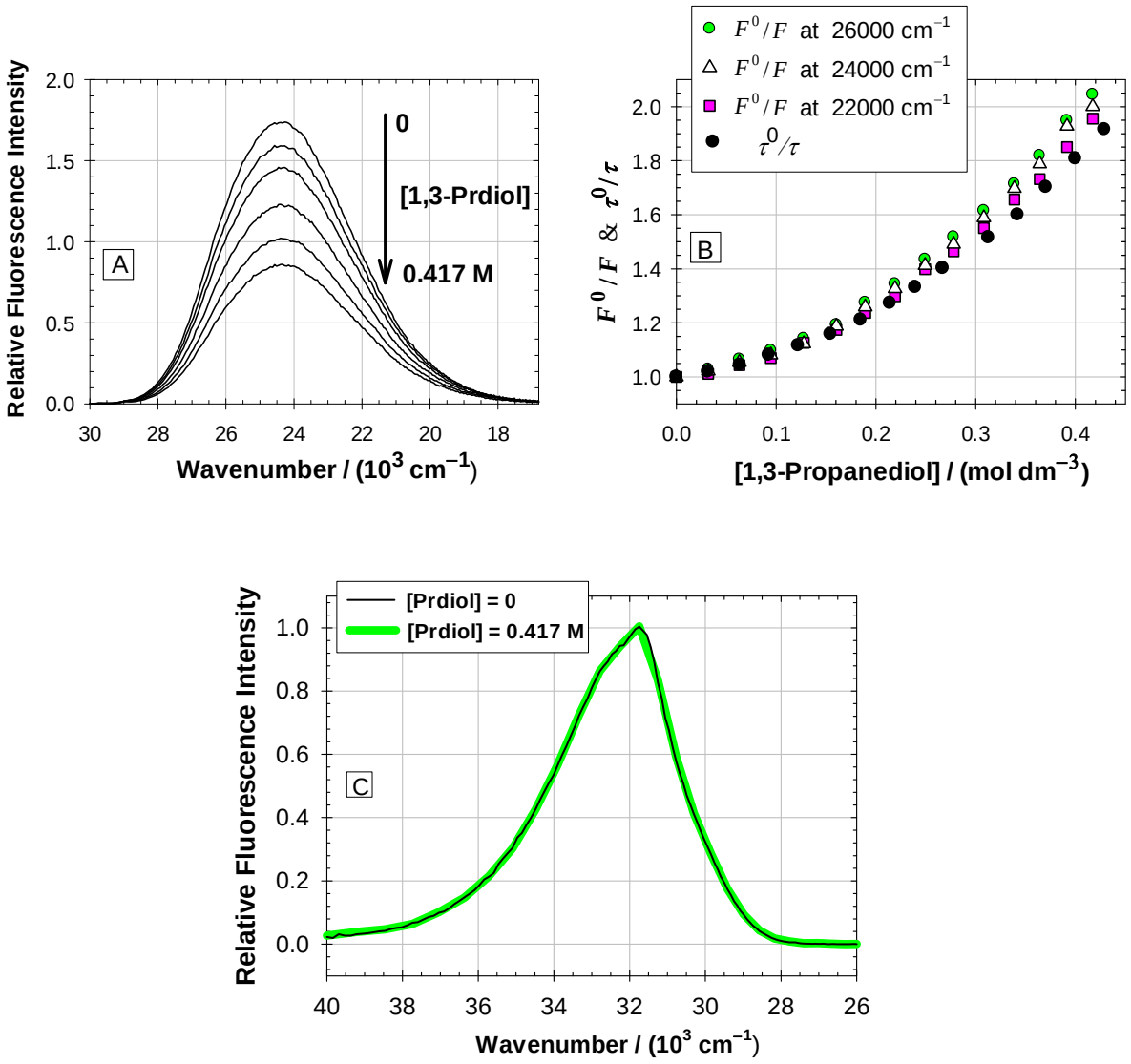

Figure 9S. Influence of 1,3-propanediol on the fluorescence spectra of $\mathbf{MQ^+}$ in acetonitrile: (A) Fluorescence emission spectra with increasing concentration of 1,3-propanediol in the range 0 to 0.417 mol/dm^3 ($\tilde{\nu}_{\mathbf{exc}}$ = 31950 cm^{-1}); (B) Influence of 1,3-propanediol concentration on the fluorescence intensity ratio F^0/F at various emission wavenumbers ($\tilde{\nu}_{\mathbf{exc}}$ = 31950 cm^{-1}), and on the fluorescence lifetime ratio τ^0/τ ($\tilde{\nu}_{\mathbf{exc}}$ = 32450 cm^{-1}, $\tilde{\nu}_{\mathbf{em}}$ = 24400 cm^{-1}); (C) Normalized fluorescence excitation spectra in pure acetonitrile and with addition of 0.417 mol/dm^3 of 1,3-propanediol ($\tilde{\nu}_{\mathbf{em}}$ = 24630 cm^{-1}). [$\mathbf{MQ^+}$] = 7.52 × 10^{-6} mol/dm^3 for the steady-state measurements and 9.96 × 10^{-5} mol/dm^3 for the lifetime measurements.

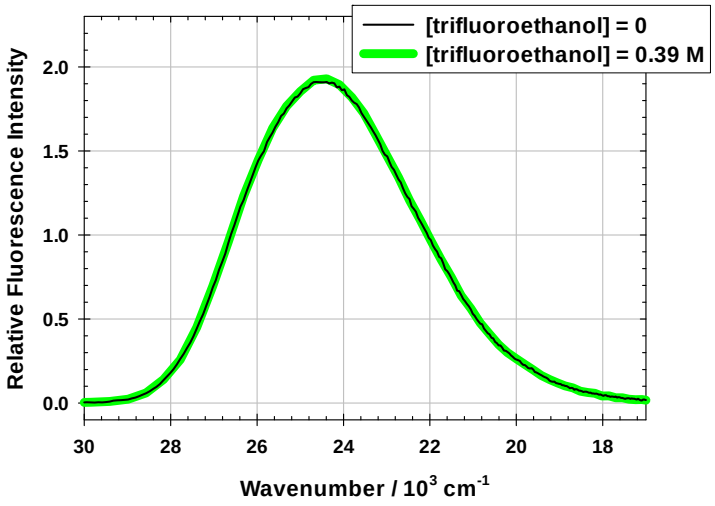

Figure 10S. Fluorescence emission spectra of the N-methylquinolinium cation in neat acetonitrile and with addition of 0.39 M of 2,2,2-trifluoroethanol. The spectra were not normalized. [$\mathbf{MQ}^+$] = 9.01×10^{-6} M. $\tilde{\nu}_{excitation}$ = 31950 cm^{-1}.

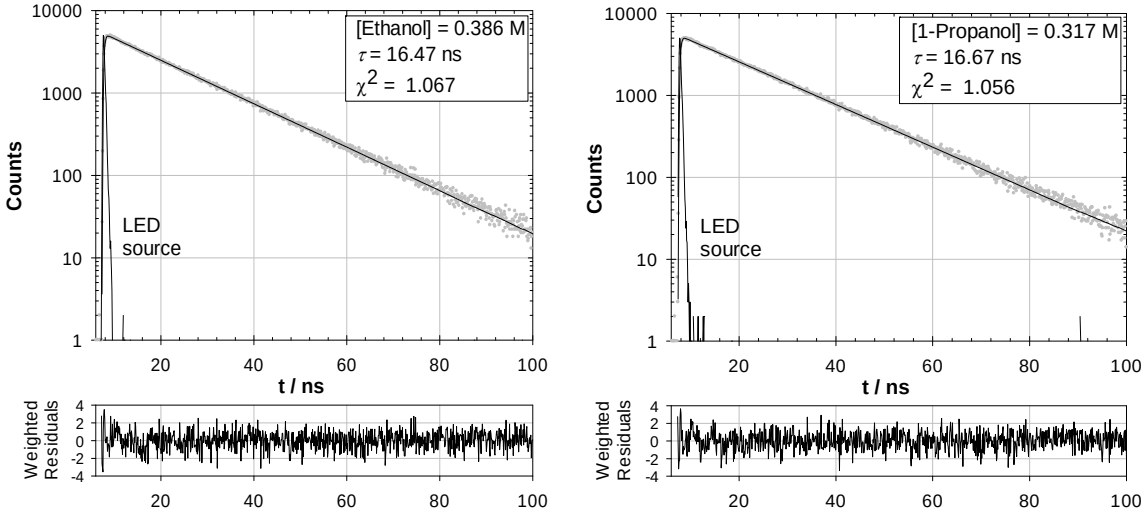

Figure 11S. Fluorescence decay of the N-methylquinolinium cation in acetonitrile with addition of 0.386 M ethanol (left, [$\mathbf{MQ}^+$] = 1.02×10^{-4} M) and 0.317 M 1-propanol (right, [$\mathbf{MQ}^+$] = 1.00×10^{-4} M), and LED source profile. The monoexponential fit and the weighted residuals are also shown. $\tilde{\nu}_{excitation}$ = 32450 cm^{-1}. $\tilde{\nu}_{emission}$ = 24400 cm^{-1}.

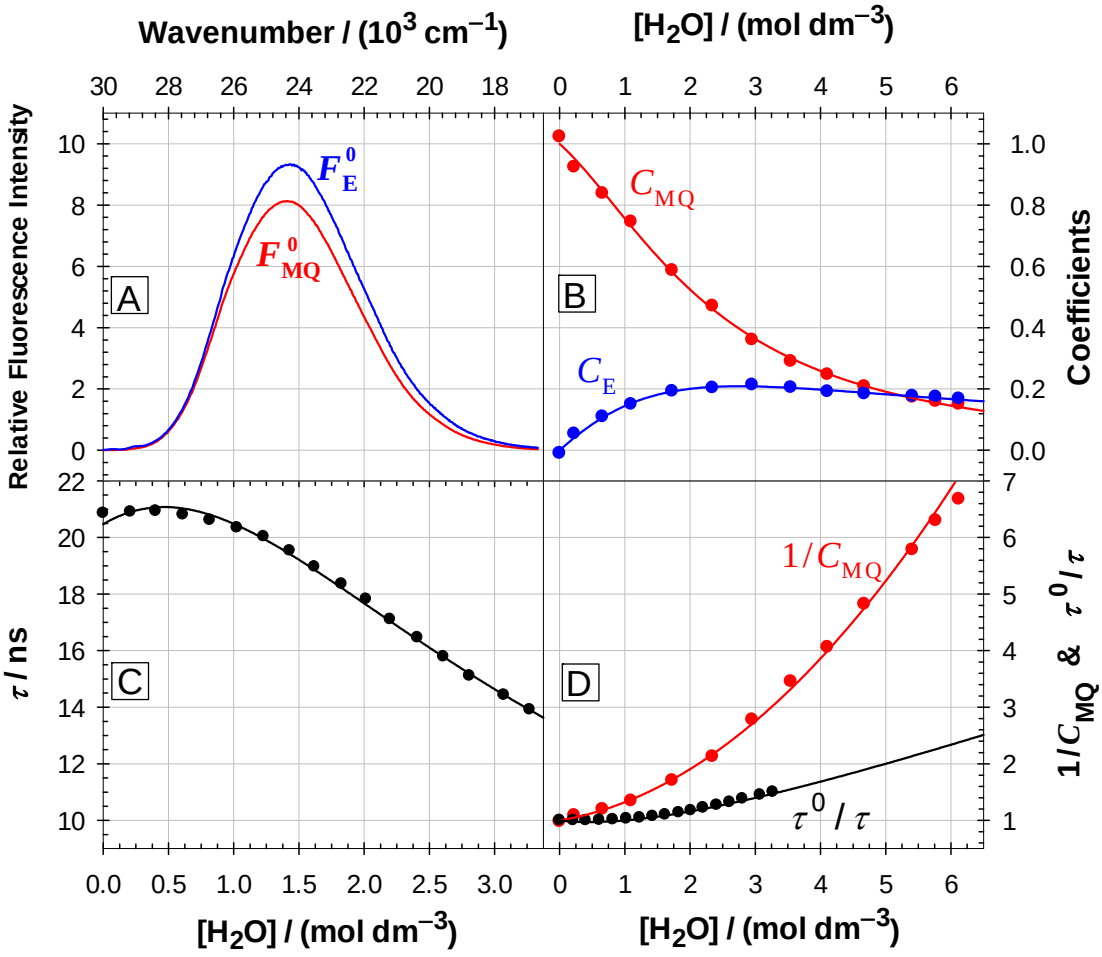

Figure 12S. Results of the principal component global analysis of the fluorescence spectra and lifetimes of $\mathbf{MQ}^+$ in acetonitrile in the presence of water: (A) Component spectra obtained, associated to $\mathbf{MQ}^{+}\mathbf{*}$ ($\boldsymbol{F}^0_{\mathrm{MQ}}$) and the exciplex ($\boldsymbol{F}^0_{\mathrm{E}}$); (B) the coefficients C_{MQ} and C_{E} representing the contributions of $\mathbf{MQ}^{+}\mathbf{*}$ and **E*** spectra to the experimental spectrum, and the fit lines; (C) the experimental fluorescence lifetimes and the fit line; (D) the experimental values of $1/C_{\mathrm{MQ}}$ and τ^0/τ, and the calculated fits.

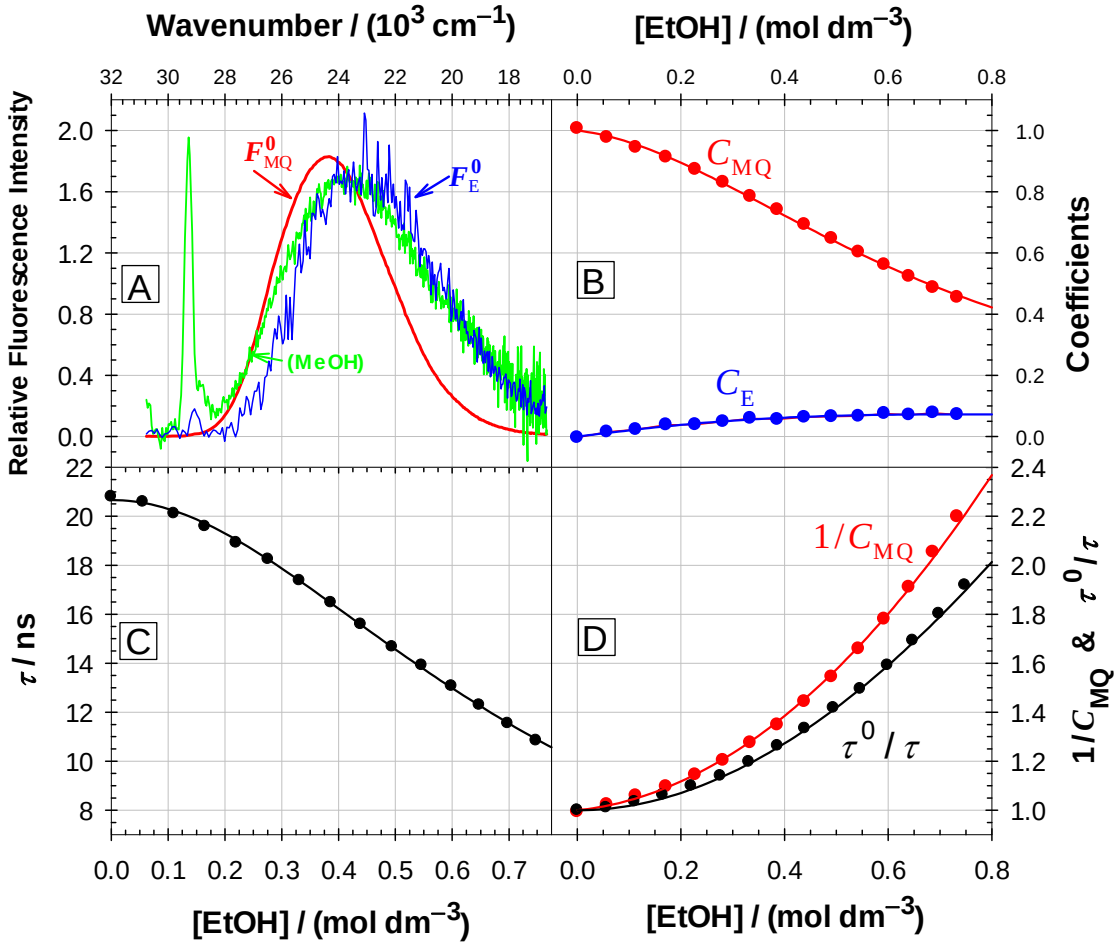

Figure 13S. Results of the principal-component global analysis of the fluorescence spectra and lifetimes of $\mathbf{MQ}^+$ in acetonitrile in the presence of ethanol: (A) Normalized component spectra obtained, associated to $\mathbf{MQ}^{+}\mathbf{*}$ (F'^{0}_{MQ}, red line) and the exciplex (F^{0}_{E}, blue line), together with the fluorescence spectrum of $\mathbf{MQ}^+$ in neat ethanol ($\tilde{\nu}_{excitation}$ = 31950 cm^{-1}, green line, with solvent Raman band); (B) the coefficients C_{MQ} and C_E representing the contributions of $\mathbf{MQ}^{+}\mathbf{*}$ and **E*** spectra to the experimental spectrum, and the fit lines; (C) the experimental fluorescence lifetimes and the fit line; (D) the experimental values of $1/C_{MQ}$ and τ^0/τ, and the calculated fits.

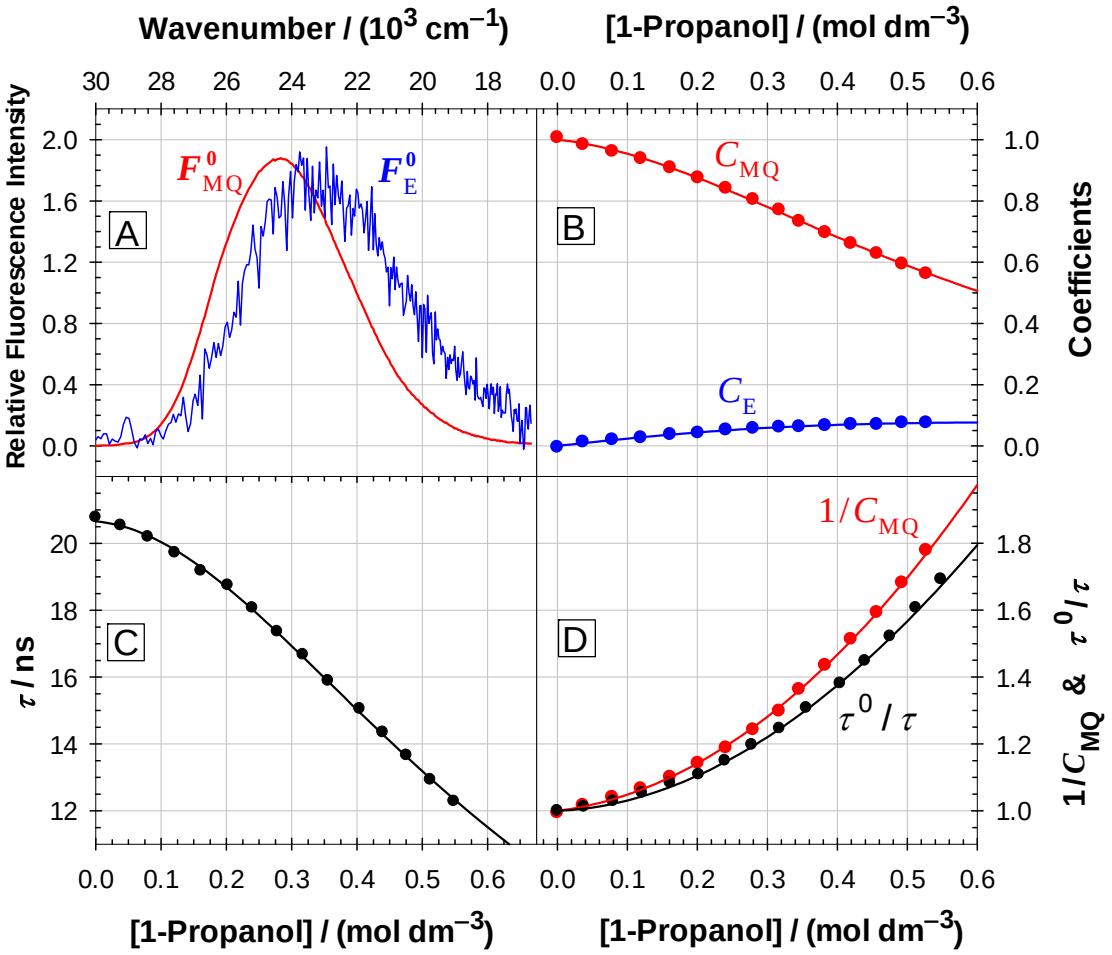

Figure 14S. Results of the principal component global analysis of the fluorescence spectra and lifetimes of $\mathbf{MQ}^+$ in acetonitrile in the presence of 1-propanol: (A) Normalized component spectra obtained, associated to $\mathbf{MQ}^{+}\mathbf{*}$ ($\boldsymbol{F}^0_{\mathrm{MQ}}$) and the exciplex ($\boldsymbol{F}^0_{\mathrm{E}}$); (B) the coefficients C_{MQ} and C_{E} representing the contributions of $\mathbf{MQ}^{+}\mathbf{*}$ and **E*** spectra to the experimental spectrum, and the fit lines; (C) the experimental fluorescence lifetimes and the fit line; (D) the experimental values of $1/C_{\mathrm{MQ}}$ and τ^0/τ, and the calculated fits.

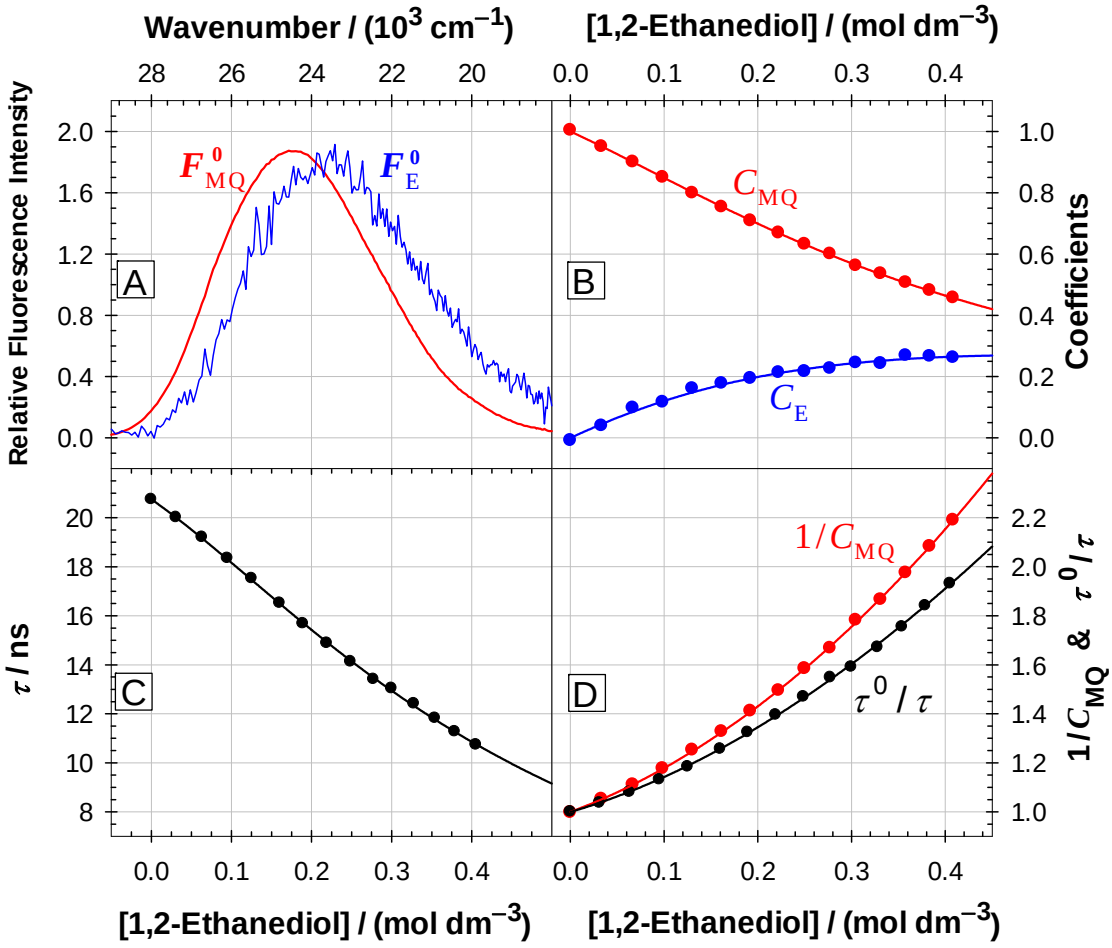

Figure 15S. Results of the principal component global analysis of the fluorescence spectra and lifetimes of $\mathbf{MQ^+}$ in acetonitrile in the presence of 1,2-ethanediol: (A) Normalized component spectra obtained, associated to $\mathbf{MQ^{+}*}$ ($\boldsymbol{F}^0_{MQ}$) and the exciplex ($\boldsymbol{F}^0_E$); (B) the coefficients C_{MQ} and C_E representing the contributions of $\mathbf{MQ^{+}*}$ and **E*** spectra to the experimental spectrum, and the fit lines; (C) the experimental fluorescence lifetimes and the fit line; (D) the experimental values of $1/C_{MQ}$ and τ^0/τ, and the calculated fits.

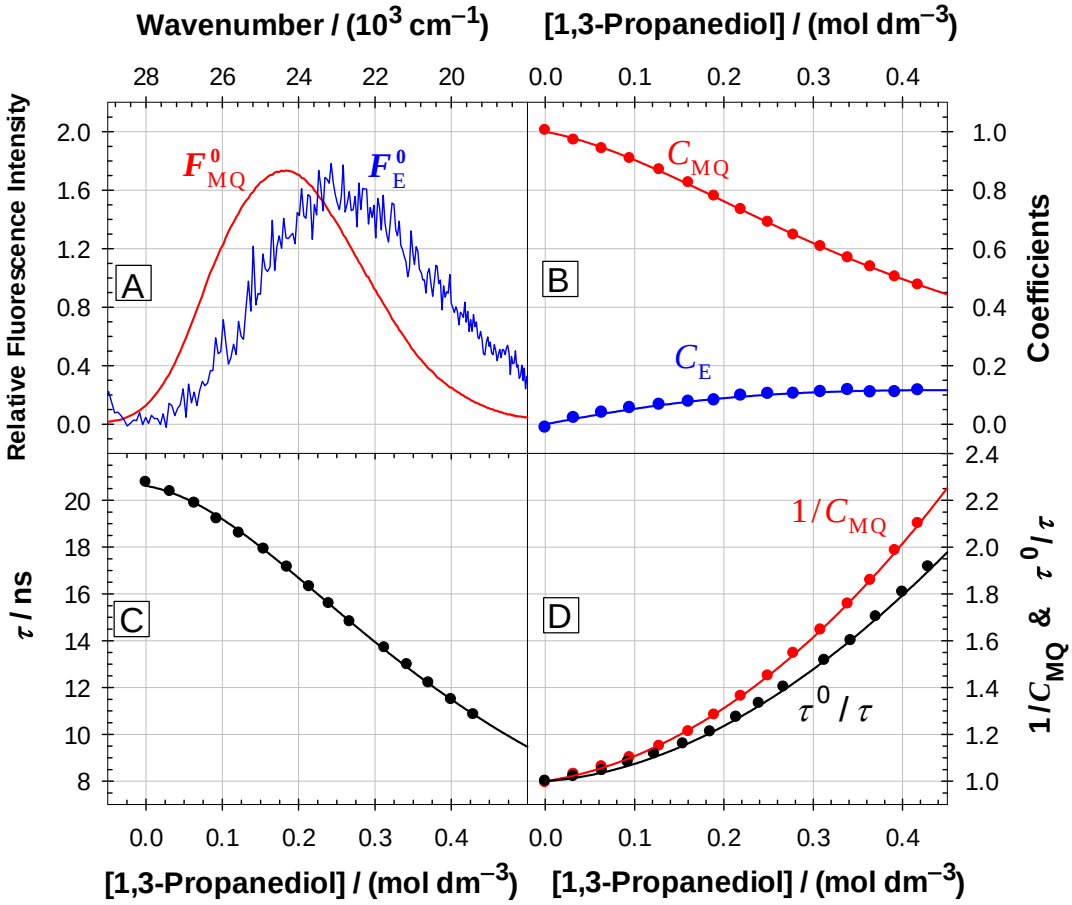

Figure 16S. Results of the principal component global analysis of the fluorescence spectra and lifetimes of $\mathbf{MQ}^+$ in acetonitrile in the presence of 1,3-propanediol: (A) Normalized component spectra obtained, associated to $\mathbf{MQ}^{+}\mathbf{*}$ ($\boldsymbol{F}^0_{\mathrm{MQ}}$) and the exciplex ($\boldsymbol{F}^0_{\mathrm{E}}$); (B) the coefficients C_{MQ} and C_{E} representing the contributions of $\mathbf{MQ}^{+}\mathbf{*}$ and **E*** spectra to the experimental spectrum, and the fit lines; (C) the experimental fluorescence lifetimes and the fit line; (D) the experimental values of $1/C_{\mathrm{MQ}}$ and τ^0/τ, and the calculated fits.

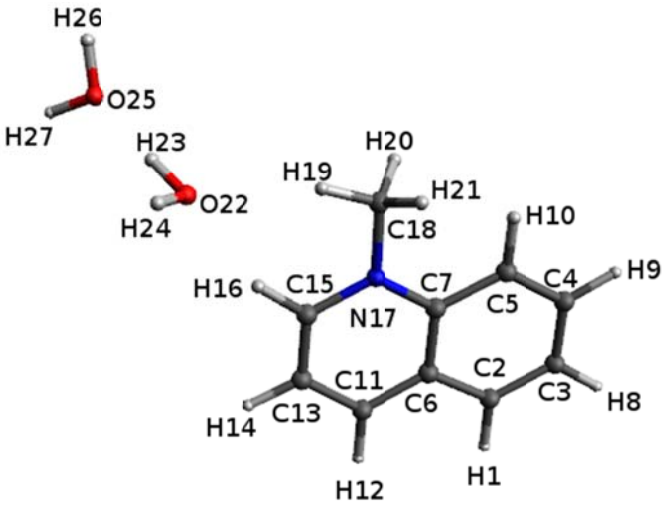

Figure 17S. Atom numbering for the complex of **MQ**$^{+}$ with two water molecules.

Table 1S. Atomic Cartesian Coordinates for the B3LYP/aug-cc-pVTZ optimized geometry of the MQ^{+}–$2H_2O$ complex in the electronic ground state

Atom number	Atom type	x/Å	y/Å	z/Å
1	H	3.791569	1.838906	0.425678
2	C	3.287986	0.888509	0.314661
3	C	3.984654	–0.287867	0.389893
4	C	3.309775	–1.514386	0.243322
5	C	1.952987	–1.562768	0.023374
6	C	1.891709	0.883707	0.089751
7	C	1.222554	–0.364952	–0.057518
8	H	5.051285	–0.280833	0.561722
9	H	3.866862	–2.438721	0.304412
10	H	1.465598	–2.517880	–0.084444
11	C	1.141622	2.073129	0.006824
12	H	1.646767	3.023417	0.118420
13	C	–0.211958	2.022136	–0.212579
14	H	–0.813185	2.915511	–0.280884
15	C	–0.833226	0.784049	–0.352758
16	H	–1.898405	0.686282	–0.528851
17	N	–0.144821	–0.356849	–0.278685
18	C	–0.877476	–1.631021	–0.439345
19	H	–1.924364	–1.403090	–0.611724
20	H	–0.771595	–2.226704	0.464435
21	H	–0.472827	–2.177144	–1.288329
22	O	–3.832914	–0.062113	–0.888846
23	H	–4.531238	–0.103405	–0.207473
24	H	–4.297994	0.015103	–1.727324
25	O	–5.759254	–0.205215	1.139786
26	H	–6.303085	–0.982769	1.302427
27	H	–6.270053	0.544671	1.461468

Table 2S. Atomic Cartesian Coordinates for the B3LYP/aug-cc-pVTZ optimized geometry of the MQ^{+}–$2H_2O$ complex in the first-excited singlet state

Atom number	Atom type	x/Å	y/Å	z/Å
1	H	3.853973	1.741623	0.427688
2	C	3.309474	0.813673	0.309308
3	C	4.029395	–0.410101	0.375715
4	C	3.347019	–1.588527	0.226544
5	C	1.953925	–1.549455	0.011637
6	C	1.910035	0.884817	0.094733
7	C	1.223286	–0.319856	–0.058559
8	H	5.096243	–0.390856	0.542048
9	H	3.850257	–2.542686	0.270111
10	H	1.426416	–2.483893	–0.102301
11	C	1.212320	2.134055	0.034674
12	H	1.741124	3.065579	0.153033
13	C	–0.166043	2.086721	–0.179255
14	H	–0.746017	2.996454	–0.232050
15	C	–0.825578	0.893589	–0.328869
16	H	–1.888753	0.813271	–0.496714
17	N	–0.137792	–0.321286	–0.273011
18	C	–0.897141	–1.562777	–0.444700
19	H	–1.937401	–1.303770	–0.618704
20	H	–0.835946	–2.182213	0.451063
21	H	–0.529125	–2.126009	–1.302965
22	O	–3.883308	–0.100237	–0.890407
23	H	–4.587889	–0.151599	–0.218470
24	H	–4.340062	0.004262	–1.730251
25	O	–5.859159	–0.267966	1.117300
26	H	–6.436725	-1.027686	1.242550
27	H	–6.341966	0.489309	1.463525